

## An infrared census of R Coronae Borealis Stars II – Spectroscopic classifications and implications for the rate of low-mass white dwarf mergers

VIRAJ R. KARAMBELKAR,<sup>1</sup> MANSI M. KASLIWAL,<sup>1</sup> PATRICK TISSERAND,<sup>2</sup> SHREYA ANAND,<sup>1</sup> MICHAEL C. B. ASHLEY,<sup>3</sup> LARS BILDSTEN,<sup>4,5</sup> GEOFFREY C. CLAYTON,<sup>6,7</sup> COURTNEY C. CRAWFORD,<sup>8</sup> KISHALAY DE,<sup>9,\*</sup> NICHOLAS EARLEY,<sup>1</sup> MATTHEW J. HANKINS,<sup>10</sup> XANDER HALL,<sup>1</sup> ASTRID LAMBERTS,<sup>11,12</sup> RYAN M. LAU,<sup>13</sup> DAN MCKENNA,<sup>14</sup> ANNA MOORE,<sup>15</sup> ERAN O. OFEK,<sup>16</sup> ROGER M. SMITH,<sup>14</sup> ROBERTO SORIA,<sup>17,18,19</sup> JAMIE SOON,<sup>15</sup> AND TONY TRAVOUILLON<sup>15</sup>

<sup>1</sup>*Cahill Center for Astrophysics, California Institute of Technology, Pasadena, CA 91125, USA*

<sup>2</sup>*Sorbonne Université, CNRS, UMR 7095, Institut d'Astrophysique de Paris, 98 bis bd Arago, 75014 Paris, France*

<sup>3</sup>*School of Physics, University of New South Wales, Sydney, NSW 2052, Australia*

<sup>4</sup>*Department of Physics, University of California, Santa Barbara, CA 93106, USA*

<sup>5</sup>*Kavli Institute for Theoretical Physics, University of California, Santa Barbara, CA 93106, USA*

<sup>6</sup>*Department of Physics & Astronomy, Louisiana State University, Baton Rouge, LA 70803, USA*

<sup>7</sup>*Space Science Institute, 4765 Walnut St, Suite B Boulder, CO 80301, USA*

<sup>8</sup>*Sydney Institute for Astronomy (SIFA), School of Physics, University of Sydney, Sydney, NSW 2006, Australia*

<sup>9</sup>*MIT-Kavli Institute for Astrophysics and Space Research, 77 Massachusetts Ave., Cambridge, MA 02139, USA*

<sup>10</sup>*Arkansas Tech University, Russellville, AR 72801, USA*

<sup>11</sup>*Laboratoire Lagrange, Université Cote d'Azur, Observatoire de la Cote d'Azur, CNRS, Bd de l'Observatoire, 06300 Nice, France*

<sup>12</sup>*Laboratoire Artemis, Université Cote d'Azur, Observatoire de la Cote d'Azur, CNRS, Bd de l'Observatoire, 06300 Nice, France*

<sup>13</sup>*NSF's National Optical-Infrared Astronomy Research Laboratory, 950 N. Cherry Ave., Tucson, AZ 85719, USA*

<sup>14</sup>*Caltech Optical Observatories, California Institute of Technology, Pasadena, CA 91125, USA*

<sup>15</sup>*Research School of Astronomy and Astrophysics, Australian National University, Canberra, ACT 2611, Australia*

<sup>16</sup>*Department of Particle Physics and Astrophysics, Weizmann Institute of Science, Rehovot 76100, Israel*

<sup>17</sup>*College of Astronomy and Space Sciences, University of the Chinese Academy of Sciences, Beijing 100049, China*

<sup>18</sup>*INAF-Osservatorio Astrofisico di Torino, Strada Osservatorio 20, I-10025 Pino Torinese, Italy*

<sup>19</sup>*Sydney Institute for Astronomy, School of Physics A28, The University of Sydney, Sydney, NSW 2006, Australia*

### ABSTRACT

We present results from a systematic infrared (IR) census of R Coronae Borealis (RCB) stars in the Milky Way, using data from the Palomar Gattini IR (PGIR) survey. R Coronae Borealis stars are dusty, erratic variable stars presumably formed from the merger of a He-core and a CO-core white dwarf (WD). PGIR is a 30 cm  $J$ -band telescope with a 25 deg<sup>2</sup> camera that surveys 18000 deg<sup>2</sup> of the northern sky ( $\delta > -28^\circ$ ) at a cadence of 2 days. Using PGIR  $J$ -band lightcurves for  $\sim 60$  million stars together with mid-IR colors from WISE, we selected a sample of 530 candidate RCB stars. We obtained near-IR spectra for these candidates and identified 53 RCB stars in our sample. Accounting for our selection criteria, we find that there are a total of  $\approx 350^{+150}_{-100}$  RCB stars in the Milky Way. Assuming typical RCB lifetimes, this corresponds to an RCB formation rate of  $0.8 - 5 \times 10^{-3} \text{ yr}^{-1}$ , consistent with observational and theoretical estimates of the He-CO WD merger rate. We searched for quasi-periodic pulsations in the PGIR lightcurves of RCB stars and present pulsation periods for 16 RCB stars. We also examined high-cadenced *TESS* lightcurves for RCB and the chemically similar, but dustless hydrogen-deficient carbon (dLHdC) stars. We find that dLHdC stars show variations on timescales shorter than RCB stars, suggesting that they may have lower masses than RCB stars. Finally, we identified 3 new spectroscopically confirmed and 12 candidate Galactic DY Per type stars – believed to be colder cousins of RCB star – doubling the sample of Galactic DY Per type stars.

## 1. INTRODUCTION

R Coronae Borealis (RCB) stars are an enigmatic class of stellar variables, notable for extreme brightness variations and peculiar chemical compositions (Clayton 2012). They show deep, rapid declines in their optical brightness ( $\lesssim 9$  mag in  $V$  band), which can last hundreds of days before rising back to their initial state (Clayton 1996). In addition, they have helium-rich atmospheres with an acute deficiency of hydrogen and an overabundance of carbon (Asplund et al. 2000). The chemical compositions of RCB stars point to them being remnants of white dwarf (WD) mergers between a He-WD and a CO-WD (Webbink 1984; Clayton et al. 2005, 2007), possibly making them low-mass analogs of type Ia supernova progenitors (Fryer & Diehl 2008). Furthermore, close He-CO WD binaries are expected to be the dominant population of gravitational wave sources detected by LISA (Lamberts et al. 2019). RCB stars represent the fate of this population and can potentially be used to infer the merger rates of these.

RCB stars have several intriguing properties that present challenges to models of stellar evolution. Their photometric declines are the result of mass-loss episodes that produce dust and obscure the star (Clayton et al. 1992). The origin of these mass-loss episodes is still not known. While at maximum light, some RCB stars pulsate with periods between 40–100 days (Lawson & Cottrell 1997), with the pulsation periods likely depending on their effective temperatures ( $T_{\text{eff}}$ ) which range from 4000 – 8000 K (Tisserand et al. 2024b; Crawford et al. 2023). The origin of these pulsations is still not known – they have been attributed either to the strange-mode instability (Saio 2008; Gautschy 2023), or thought to be solar-like oscillations in helium-rich envelopes (Wong & Bildsten 2024).

RCB stars are closely related to the class of dustless Hydrogen-deficient Carbon stars (dLHdC stars, Warner 1967; Tisserand et al. 2022). dLHdC stars have similar chemical compositions to RCB stars, but show no signs of dust-formation. Together, RCB and dLHdC stars constitute the class of Hydrogen-deficient Carbon (HdC) stars. The differences between RCB stars and dLHdC stars have been explored only recently, based on their positions in the HR diagram (Tisserand et al. 2022), their oxygen isotope ratios (Karambelkar et al. 2022), their strontium-abundances (Crawford et al. 2022) and

their H and Li content (Crawford et al. 2023). These initial results suggest that RCB stars may be more massive than dLHdC stars. These results are based on small samples of these stars, and it still remains a mystery as to why RCB stars form dust, while dLHdC stars do not.

A third class of stars called DY Per type stars is thought to be a colder sub-class of RCB stars (with  $T_{\text{eff}} \approx 3500$  K), marked by shallower and more symmetric declines in their lightcurves (Alcock et al. 2001). Only 3 DY Per type stars have been confirmed in the Milky Way (Tisserand et al. 2008, 2013), while about a dozen have been confirmed in the Magellanic Clouds (Alcock et al. 2001; Tisserand et al. 2004, 2009). These stars have a hydrogen-deficiency, a high carbon-abundance (Začs et al. 2007) and have been recently found to have a high  $^{18}\text{O}$  abundance (Bhowmick et al. 2018; García-Hernández et al. 2023) – resembling RCB stars. On the other hand, their luminosities and infrared colors are very similar to cool N-type carbon stars and differ significantly from RCB stars (Alcock et al. 2001; Soszyński et al. 2009; Tisserand et al. 2009). It is debated whether DY Per type stars are colder RCB stars originating in WD mergers, or classical carbon stars undergoing strong dust-formation.

When RCB stars are enshrouded by dust, they appear brighter at infrared wavelengths than the optical (Feast 1997). The photometric declines are also shallower in the infrared ( $\lesssim 3$  mag in  $J$ -band) than in the optical (Karambelkar et al. 2021). Despite this, most previous searches for RCB stars have focused on optical surveys such as MACHO (Alcock et al. 2001; Zaniewski et al. 2005), OGLE (Tisserand et al. 2011), EROS-2 (Tisserand et al. 2004, 2008, 2009), the Catalina Survey (Lee 2015), All Sky Automated Survey for Supernovae (ASASSN, Tisserand et al. 2013; Shields et al. 2019; Otero et al. 2014), the Palomar Transient Facility (Tang et al. 2013) and the Zwicky Transient Facility (Lee et al. 2020).

The first IR-search for RCB stars was carried out by Tisserand (2012), who used WISE and 2MASS colors to publish a list of RCB candidates. Tisserand et al. (2020) subsequently refined the selection criteria and published a catalog of 2356 RCB candidates and 40 new RCB stars confirmed via optical spectroscopy, suggesting that there are 300 – 500 RCB stars in the Milky Way. In our previous paper (Karambelkar et al. 2021), near-IR (NIR)  $J$ -band lightcurves from Palomar Gattini IR (De et al. 2020) together with WISE colors yielded 394 promising

\* NASA Einstein Fellow

candidates for spectroscopic follow-up. Using NIR spectra for a 26 of these, 11 new RCB stars were presented.

In this paper, we complete the NIR census of RCB stars and present NIR spectra (1–2.4  $\mu\text{m}$ ) of the full sample of RCB candidates listed in [Karambelkar et al. \(2021\)](#). Additionally, we conduct a WISE-color independent search for RCB stars using PGIR lightcurves to find RCB stars missed by the color-selection criteria. We also use the PGIR lightcurves to search for new DY Per type stars in the Milky Way. We describe our candidate selection criteria in Section 2, the NIR spectroscopic observations in Section 3 and the classifications in Section 4. We use this complete census of RCB stars to derive the total number of RCB stars expected in the Milky Way and infer the rate of He and CO white dwarf mergers in Section 5. We use the NIR spectra and lightcurves to measure their radial velocities, their positions in the color-magnitude diagram and pulsation periods. We also examine high cadenced *TESS* lightcurves of a sample of RCB and dLHdC stars. We conclude with a summary of our results in Section 6

## 2. CANDIDATE SELECTION

### 2.1. *IR color + PGIR lightcurve - based selection*

Our candidate selection is described in detail in [Karambelkar et al. \(2021\)](#). Briefly, we re-prioritize the WISE color-selected catalog of 2194 RCB candidates from [Tisserand et al. \(2020\)](#) (T20 catalog hereafter) using PGIR light-curves. First, we exclude 304 candidates that show large-amplitude periodic variations resembling AGB stars and 23 candidates whose lightcurves resemble those of RV-Tauri stars. Of the remaining candidates, we identify 177 candidates that show significant, non-periodic variations in their lightcurves, 230 candidates that show no significant variations and 253 candidates where the lightcurve is ambiguous (i.e. shows some variations that are not obviously periodic or large-amplitude). Using the location of known RCBs and LPVs in the WISE and 2MASS color diagrams, we further sub-divide Priorities A, B, C and D into seven color-based sub-categories. We prioritize categories A, 1-a, 2-a and 3-a comprising 383 candidates in total for spectroscopic follow-up.

The top panel of Fig. 1 shows a table with the distribution of candidates in these categories. This table differs slightly from the one presented in [Karambelkar et al. \(2021\)](#), as we updated the lightcurve-based priorities based on more recent PGIR *J*-band lightcurves with additional  $\approx 1.5$  years of data. The categories prioritized for NIR spectroscopic followup are marked in green. We also indicate the number of candidates for which we obtained NIR spectra in each category, and the number of

RCB stars spectroscopically confirmed within each category (by red numbers). The bottom panel of Fig. 1 shows a pie-chart with the spectroscopic classifications of all sources we observed (discussed in Sec. 4.)

As the color-criteria were chosen to search for RCB stars, we do not expect to find any DY Per type stars in this category.

### 2.2. *Color independent PGIR lightcurve-based selection*

To search for possible RCB stars missed by the T20 color-selected catalog, we searched for RCB stars in the PGIR lightcurve database, independent of any color-criteria. The PGIR lightcurve database contains aperture-photometry lightcurves spanning June 2018 to July 2021 for  $\sim 70$  million stars that were detected in the PGIR reference images. We search for stars that show RCB-like large-amplitude, erratic variations in their PGIR lightcurves. Unfortunately, the completeness of the lightcurve database is not well-quantified, especially in dense Galactic fields that are limited by confusion noise. Therefore, we cannot use this lightcurve-selection alone for a systematic RCB search. Instead, we use this to search for possible populations of RCB stars missing from the T20 catalog.

For each lightcurve in the PGIR database, we calculate the von-neumann ratio ( $\eta$ , [von Neumann 1941](#)) and peak-to-peak amplitude (ptp).  $\eta$  measures the degree of correlation between successive data-points in the lightcurve, and is well-suited to identify stars showing large-amplitude variations. Non-variable stars are expected to have  $\eta$  close to 2, while smaller  $\eta$  values suggest significant correlations in successive variations. We select 1200 stars with  $\eta < 0.5$  and  $\text{ptp} > 2.5$  mag (informed by known RCB stars). We then inspect their lightcurves to reject periodic variability and select 75 stars that show large-amplitude variations and are not present in the color-selected T20 catalog for further spectroscopic follow-up. As no color-information was used in the selection, we expect to find both RCB and DY Per type stars in this category. The spectroscopic classifications of all 75 variables will be presented in a forthcoming paper ([Earley et al., in prep.](#)). Here, we focus on RCB and DY Per type stars found within these sources.

### 2.3. *PGIR lightcurves of known carbon-stars*

As RCB stars have spectral features resembling carbon stars, we examined PGIR-*J* band lightcurves for 9975 stars classified as “carbon-star” or “candidate carbon stars” on Simbad, to search for RCB-like variations in them. We were not able to obtain NIR spectra for interesting stars identified in this category. For this reason, we report them as candidate RCB and DY Per type stars in Section 4.3, pending spectroscopic confirmation.

Light curve based priorities for 1215 candidates with decl. > -28°

	Priority A RCB-like 176 / 176	Priority B ambiguous 124 / 250	Priority C flat 53 / 230	Priority D no dets. 36 / 232	Priority E RV-Tauri 9 / 23	Priority F LPV 52 / 304	Priority G Decl. < -28° 3 / 979	
IR color based priorities for 2194 candidates	1-a 252	20 / 29 / 29	6 / 34 / 34	3 / 43 / 43	3 / 27 / 27	0 / 0	1 / 9	3 / 3 / 110
	1-b 111	2 / 15 / 15	6 / 18	4 / 10	1 / 8	2 / 2	2 / 9	0 / 49
	1-c 422	9 / 19 / 19	3 / 36	0 / 32	0 / 65	0 / 0	28 / 110	0 / 160
	2-a 548	0 / 64 / 64	1 / 42 / 42	0 / 1 / 1	0 / 7 / 15	4 / 11	18 / 139	0 / 276
	2-b 439	1 / 20 / 20	1 / 59	0 / 96	0 / 39	1 / 6	1 / 21	0 / 198
	3-a 101	1 / 22 / 22	1 / 38 / 39	0 / 5 / 5	0 / 1 / 1	2 / 4	2 / 8	0 / 71
	3-b 321	0 / 7 / 7	0 / 22	0 / 43	0 / 77	0 / 0	0 / 8	0 / 115

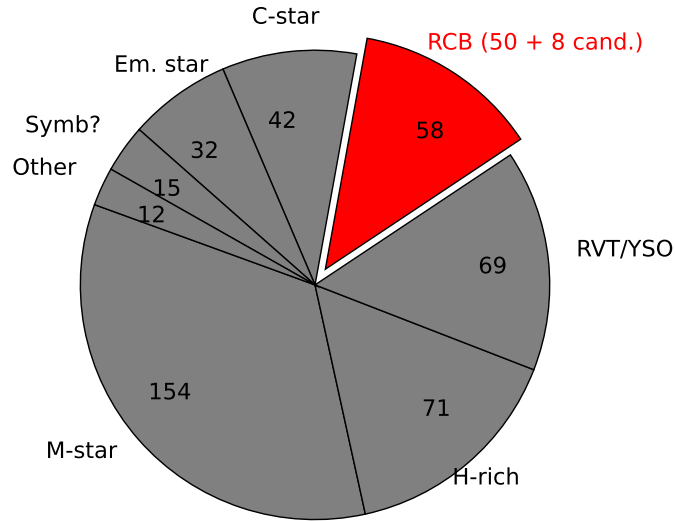


**Figure 1.** (*Top:*) Lightcurve and color-based priorities for RCB candidates (updated from Karambelkar et al. (2021) using more recent PGIR lightcurves). The categories prioritized for spectroscopic follow-up are numbered in green. In each category, we indicate the total number of candidates and the number of candidates for which we obtained NIR spectra. We also indicate the number of RCB stars identified in each category in red. We obtained NIR spectra for a total of 453 candidates. 375 of the 383 prioritized candidates have NIR spectra, corresponding to an overall completeness of  $\approx 98\%$ . 3 candidates from Priority G (decl. <  $-28^\circ$ ) were observed spectroscopically because they were listed as strong RCB candidates in T20. (*Bottom:*) Pie-chart showing our NIR spectroscopic classifications of all 453 stars.

**Table 1.** Updated priorities of WISE-selected candidates based on PGIR lightcurves

ToI-ID	RA	Dec	Priority
	deg	deg	
23	37.5679	12.28989	A
..			

**Table 2.** Spectroscopic classifications of candidates selected for followup

ToI-ID	RA	Dec	Class.	Date Inst.
	deg	deg		
23	37.5679	12.28989	RV-Tauri	
..				

### 3. NIR SPECTROSCOPIC OBSERVATIONS

We obtained medium resolution NIR spectra for a total of 453 of our color-selected candidates from the T20 catalog. This includes 375 of the 383 prioritized candidates described in Section 2.1, and 81 stars from the other priorities. All but 3 observed candidates have declination  $> -28^\circ$ . These 3 candidates belong to Priority G and were observed because they were listed as strong RCB candidates in T20. Fig. 1 shows the priority-wise distribution of stars for which we obtained NIR spectra.

The NIR spectra were obtained on several nights from October 2019 to December 2021 with the Triplespec spectrograph ( $R \approx 2700$ , Herter et al. 2008) on the 200-inch Hale telescope at Palomar Observatory and the SpeX spectrograph ( $R \approx 1500$ ) on the NASA Infrared Telescope Facility (IRTF, Rayner et al. 2003). The IRTF spectra were observed as part of programs 2020A111 and 2021B074. We obtained a total of 389 spectra with P200/Triplespec and 69 spectra with IRTF/SpeX. All spectra were extracted using the IDL package `spextool` (Cushing et al. 2004). The extracted spectra were flux calibrated and corrected for telluric absorption with standard star observations using `xtellcor` (Vacca et al. 2003).

### 4. NIR SPECTROSCOPIC CLASSIFICATIONS

We classify the 453 sources using their spectra and lightcurves. We find that these sources include a mix of RCB stars, Mira variables, carbon-rich (C-rich) AGB stars, RV Tauri stars, possible giant stars in symbiotic binaries, possible young stellar objects (YSOs) and Wolf-Rayet (WR) stars. The bottom panel of Fig. 1 shows the distribution of the source classifications. We discuss the classifications and properties of these sources

in Appendix B. Here, we focus on the sources classified as RCB stars.

As discussed in Karambelkar et al. (2021), RCB stars are characterised by the following NIR spectral features –

- RCB stars show He I ( $\lambda 10830$ ) emission or absorption. The RCB stars undergoing a photometric minimum usually show He I emission, however this can be suppressed by the circumstellar dust. The stars at or rising to maximum light show either a P-cygni profile or strong blueshifted absorption.
- RCB stars in a minimum exhibit a mostly featureless, reddened spectrum with emission lines of He I, and sometimes Si I and C<sub>2</sub>.
- At maximum light, the spectra of RCB stars resemble F-G type supergiants, with the absence or significantly weak hydrogen lines. Prominent features include absorption lines of C I (most prominently at 1.0686 and 1.0688 $\mu\text{m}$ ), Fe I, Si I and K I. Stars with cold effective ( $T_{\text{eff}} \leq 6800\text{K}$ ) temperatures show molecular absorption features due to CN (1.0875, 1.0929, 1.0966 and 1.0999 $\mu\text{m}$ ), <sup>12</sup>C<sup>16</sup>O (2.2935, 2.3227, 2.3525, 2.3829, 2.4141 $\mu\text{m}$ ) and <sup>12</sup>C<sup>18</sup>O.

#### 4.1. IR color + PGIR lightcurve - based selection

We examine our spectra and identify 74 stars that show some or all of the spectroscopic features described above. In cases where the spectra are not sufficient to determine a robust classification, we examine the lightcurves. We mainly use the PGIR *J*-band lightcurves, and also examine publicly available optical lightcurves from the Zwicky Transient Facility (ZTF, Bellm et al. 2019) and ATLAS (Tonry et al. 2018; Smith et al. 2020) surveys to search for large amplitude variations. RCB stars can also show large amplitude variations at mid-IR wavelengths due to dust formation episodes. To search for these, we use publicly available 3.6 and 4.5  $\mu\text{m}$  data from the NEOWISE survey.

First, we classified 11 of these stars as RCBs in Karambelkar et al. (2021). Of the remaining stars, 27 show RCB-like variations in the PGIR *J*-band data. We classify 26 of these as RCB stars, as the NIR spectral features are consistent with the photometric phases as suggested by the light curve. The last one – WISE-ToI-1007 shows large amplitude RCB-like variations, but does not show He I in its spectrum. As the spectrum otherwise resembles that of a carbon-star, and we suggest that this is a dust-forming carbon star and not an RCB.

26 stars do not show any large amplitude variations in PGIR data, but have spectra with features seen in

those of RCB stars. Of these, we classify 8 stars as RCB stars because their spectra very closely resemble RCB stars that haven't undergone photometric declines in a long time, or the ZTF, ATLAS or NEOWISE lightcurves show clear evidence of declines or variability in the past. Of the remaining 18 sources, the spectra of 8 show strong He emission – unlike RCB stars that haven't undergone a large-amplitude photometric decline in a long time. The ZTF and ATLAS light-curves of these 8 stars show pulsations on timescales of  $\sim 10 - 100$  days superposed on smooth longer-timescale variations, similar to those seen in RV-Tauri stars<sup>1</sup>. These 8 stars are most likely RV-Tauri stars. Of these, we highlight the source WISE-ToI-3012, as it shows a slow rise in the optical and NIR wavelengths for the last 2000 days, and shows a large amplitude dip in the NEOWISE data. The 10 remaining stars have spectra with low S/N and no conclusive features in their lightcurves to enable a confident classification. 5 of these stars show strong He emission and some strong narrow H emission lines in their spectra, suggesting that they are likely RV-Tauri stars. We list the remaining 5 – WISE-ToI-28, 41, 228, 293 and 1257 as candidate RCB stars. WISE-ToI-28 shows uncharacteristically large helium emission, but also shows periodic 1 mag variations in NEOWISE. WISE-ToI-293 shows a short timescale decline in ZTF data. WISE-ToI-41 shows weak He emission and erratic NEOWISE variations. WISE-ToI-1257 shows a steep rising red continuum with small variations in the  $J$ -band.

7 stars have no detections in the PGIR data: WISE-ToI-195, 270, 245, 288, 317, 321 and 323. Their spectra show the helium emission line. No strong hydrogen features are evident, but we cannot rule out their presence as the spectra have low S/N. Of the seven, WISE-ToI-195 and WISE-ToI-270 show RCB-like declines in their ZTF lightcurves. We classify these two as RCB stars. WISE-ToI-317 and 321 do not show any significant declines in their ZTF and ATLAS lightcurves. These two stars have distance estimates from *Gaia* (Bailer-Jones et al. 2018) which suggest that their absolute magnitudes are  $M_r \approx 4.1$  and 1.8 respectively – inconsistent with them being RCB stars. For this reason, we exclude them as RCB stars<sup>2</sup>. The remaining three – WISE-ToI-245, 288 and 323 do not show any declines in their ZTF and ATLAS lightcurves, and do not have any additional

information from *Gaia*. We list these three as strong RCB candidates.

Finally, we observed 3 stars – WISE-ToI-164, 181 and 264 – that lie outside the area covered by PGIR (i.e. have  $\delta < -28^\circ$  and belong to Priority G), but are listed as strong RCB candidates in Tisserand et al. (2020). Our NIR spectra confirm that they are RCB stars.

To summarize, we identify a total of 50 RCB stars and 8 strong RCB candidates using the PGIR-lightcurve-based prioritization of the T20 catalog. We note that of the 50 RCB stars, 19 were identified previously as RCB stars from their optical spectra by Tisserand et al. (2020). Our NIR spectra independently confirm their nature as RCBs. 6 additional RCB stars were listed as strong candidates by Tisserand et al. (2020), which we unambiguously classify as RCB stars based on their NIR spectra. Two stars WISE-ToI-185 and WISE-ToI-226 were listed as a potential RCBs based on their optical lightcurves by Eyer et al. (2023) and Maíz Apellániz et al. (2023) respectively, and are now spectroscopically classified as RCBs based on our NIR spectra. All 50 RCB stars identified or confirmed by our NIR spectra are listed in Table 3 and 4. The PGIR lightcurves of the 45 RCB stars that have PGIR detections are plotted in Figures 2, 3. The NIR spectra of all 50 RCB stars are plotted in Figures 4 and 5. The 8 strong RCB candidates are listed in Table 8, and their lightcurves and spectra are shown in Fig. 11.

## 4.2. Color-independent, PGIR lightcurve-only selection

### 4.2.1. New RCB stars

Of the 75 lightcurve-selected candidates, we identify 2 new RCB stars PGIRV663-2-3-2970 (PGIRV663 hereafter) and PGIRV526-1-0-2033 (PGIRV526 hereafter). Their lightcurves and spectra are included in Fig. 3 and 5 respectively. The  $J$ -band lightcurves of both these stars shows a slow rise of  $\approx 3$  mag over 1500 days. The ZTF lightcurve of PGIRV663 shows a 2 mag. decline, 1700 days prior to the epoch of our NIR spectrum. Based on the ZTF lightcurve, this candidate was flagged as a possible RCB star on AAVSO by G. Murakawski. The NIR spectra of both stars are similar to RCB stars that are recovering from a photometric decline, consistent with their lightcurves. Both stars have WISE and 2MASS detections, but were missed by the color-selection criteria of Tisserand et al. (2020). PGIRV526 has  $W2 - W3 = 0.85$  – failing the criterion  $W2 - W3 > 1.1$  mag, suggesting that it has hot dust ( $T > 1000$  K) around it. PGIRV663 has  $J - H = 0.70$  and  $H - K = 0.43$  mag, failing the criterion  $J - H < (H - K) + 0.2$  – suggesting that it is a warm RCB star with a thin dust shell.

<sup>1</sup> [https://ogle.astrouw.edu.pl/atlas/RV\\_Tau.html](https://ogle.astrouw.edu.pl/atlas/RV_Tau.html)

<sup>2</sup> We note that the significance of the *Gaia* parallax measurement for WISE-ToI-317 is low ( $\text{Plx}/e\text{-Plx} = 2.9$ ). Nevertheless, there is no compelling evidence, so we do not classify this as an RCB star.

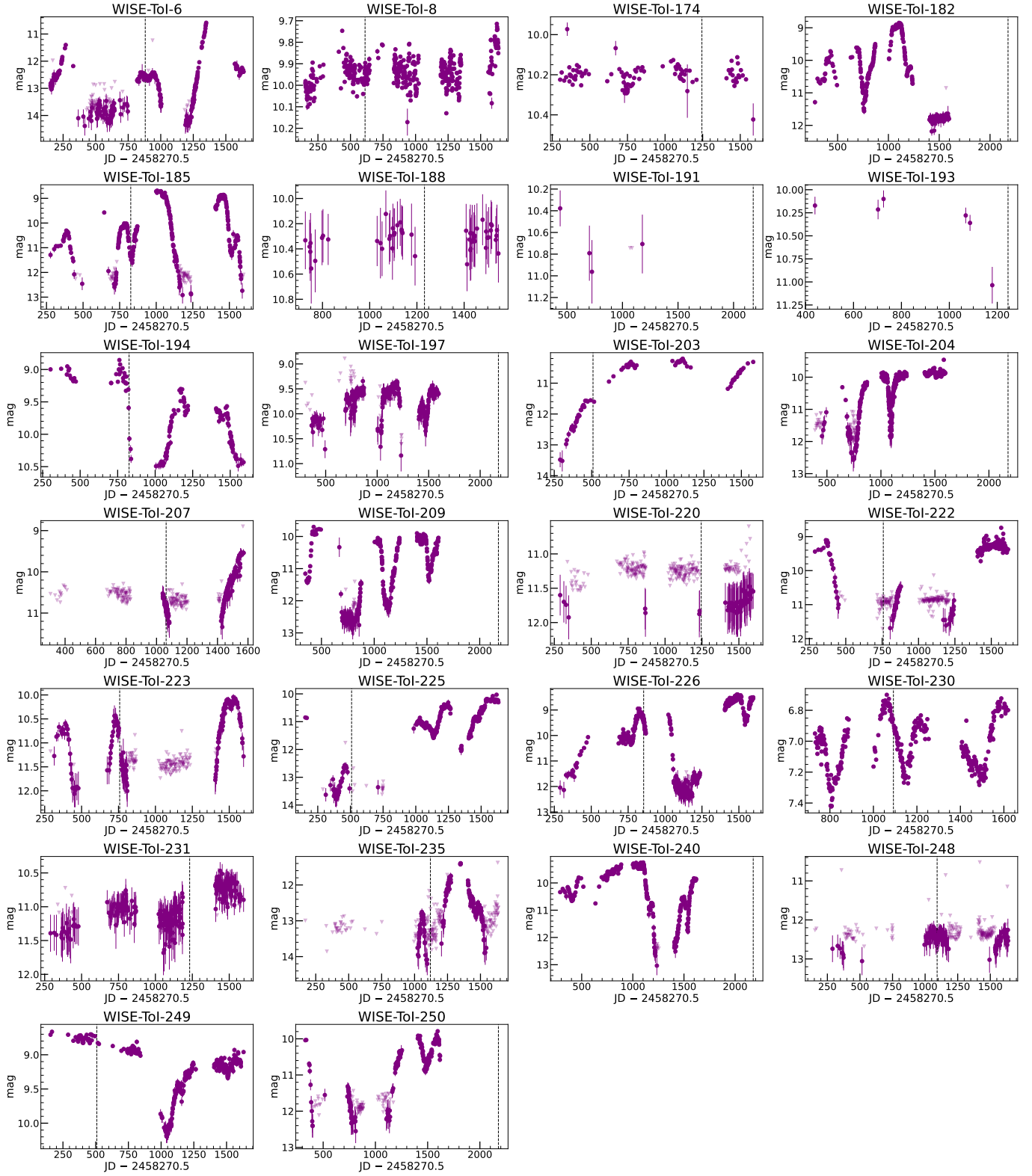


**Figure 2.** PGIR *J*-band lightcurves of new RCB stars. Circles denote detections, while triangles denote upper limits (continued in Fig. 3). The dotted black vertical line marks the epoch when the NIR spectrum was obtained.

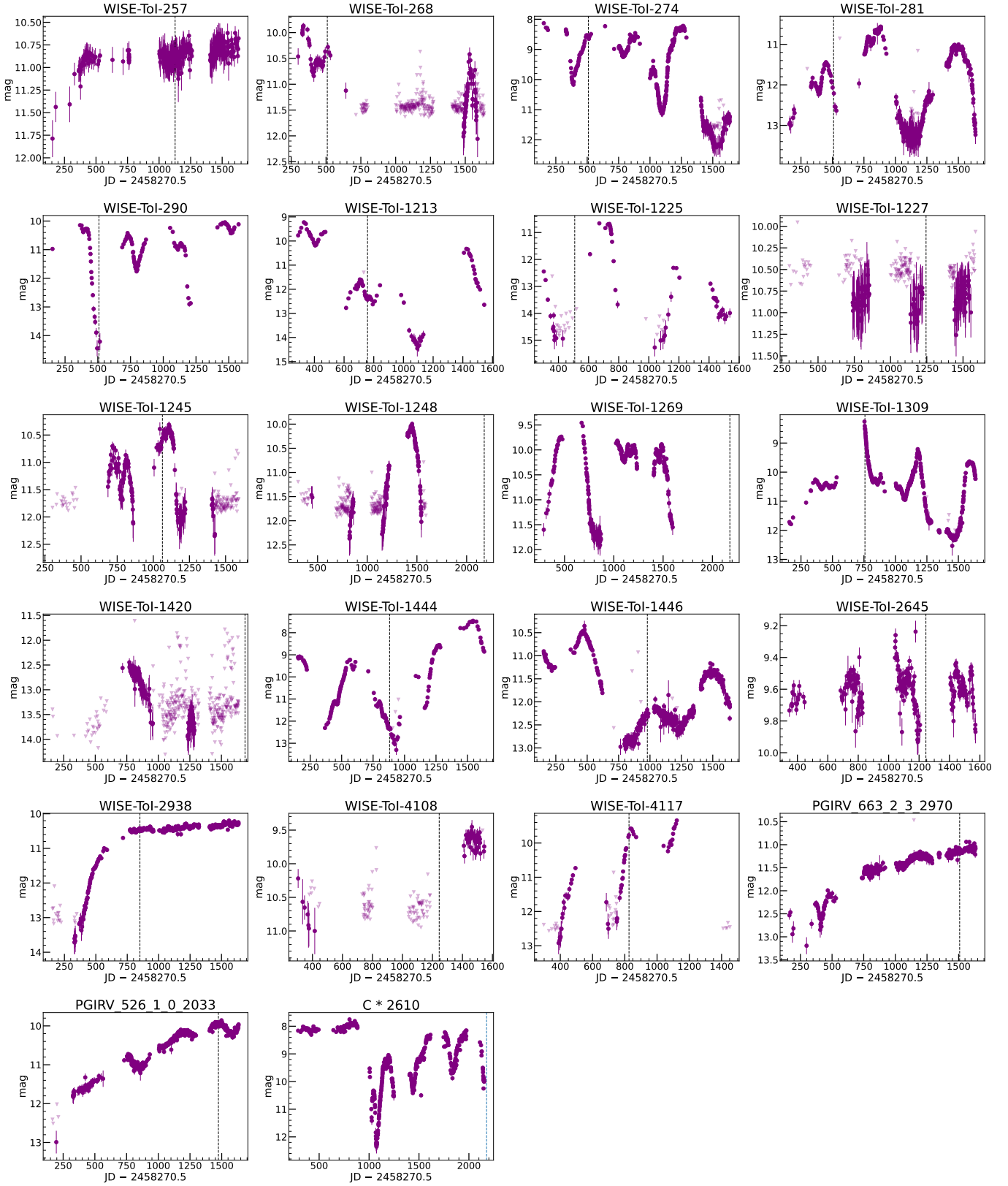


Figure 3. PGIR *J*-band lightcurves of new RCB stars



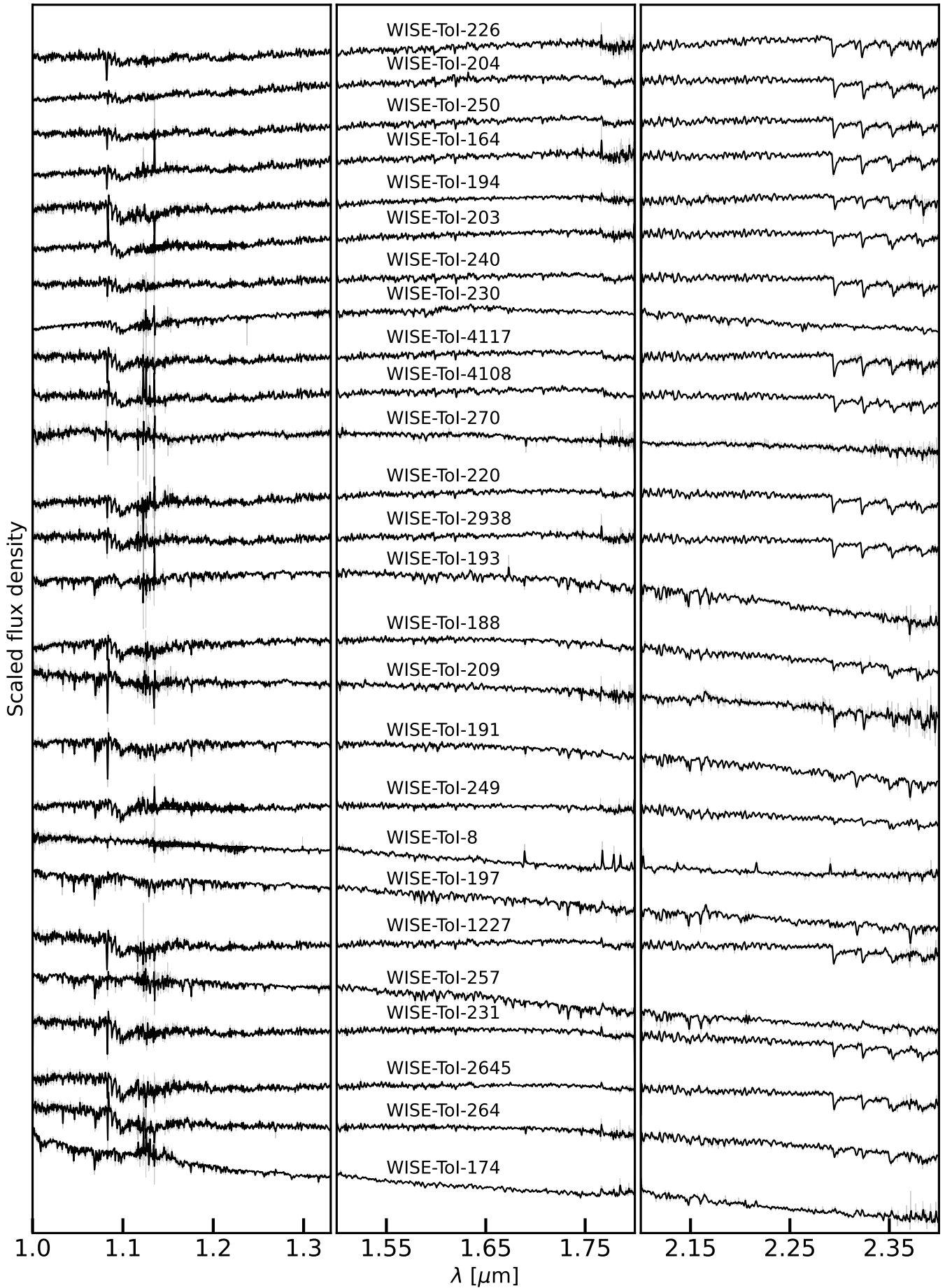


Figure 4. NIR spectra of new RCB stars

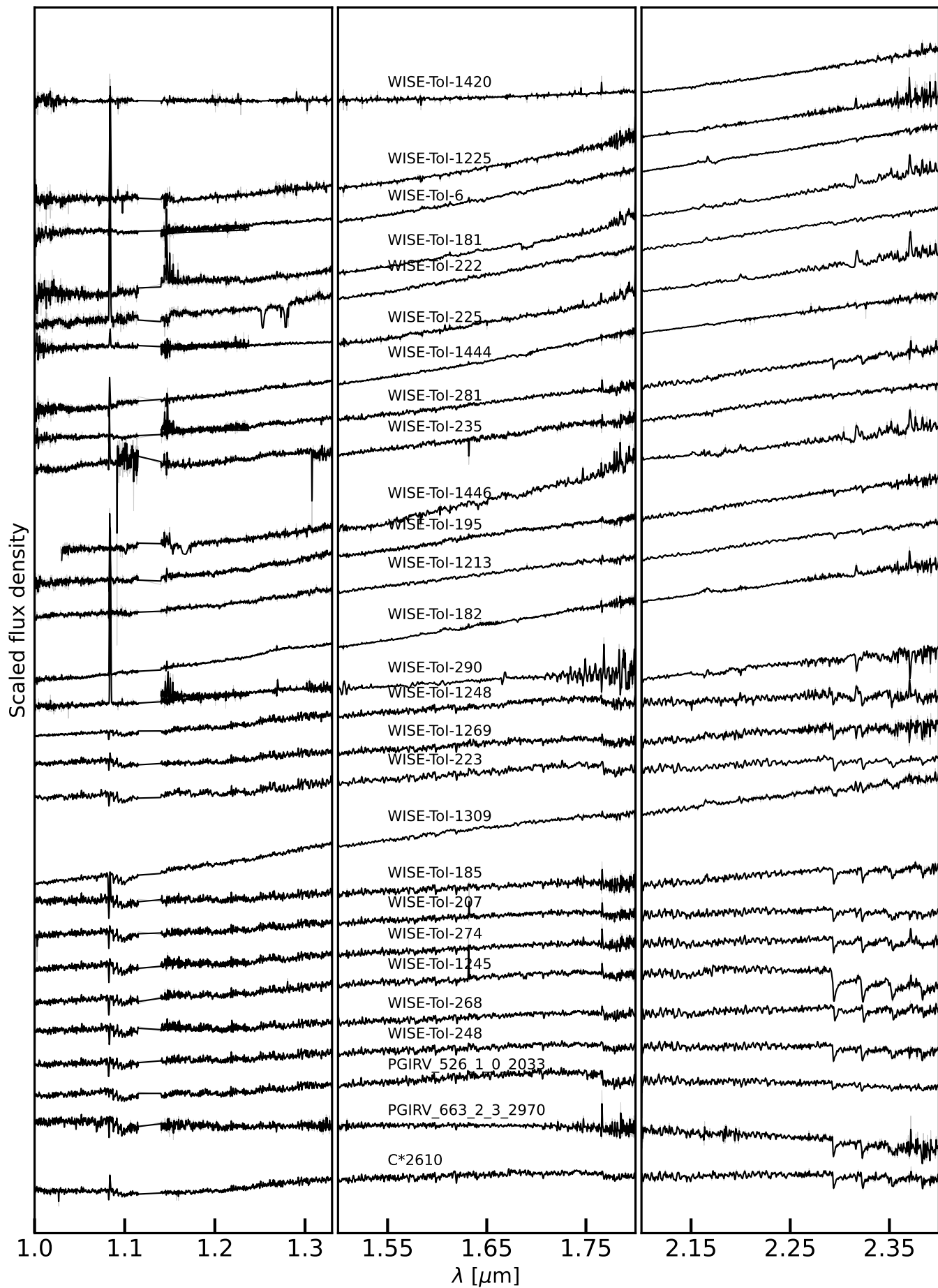
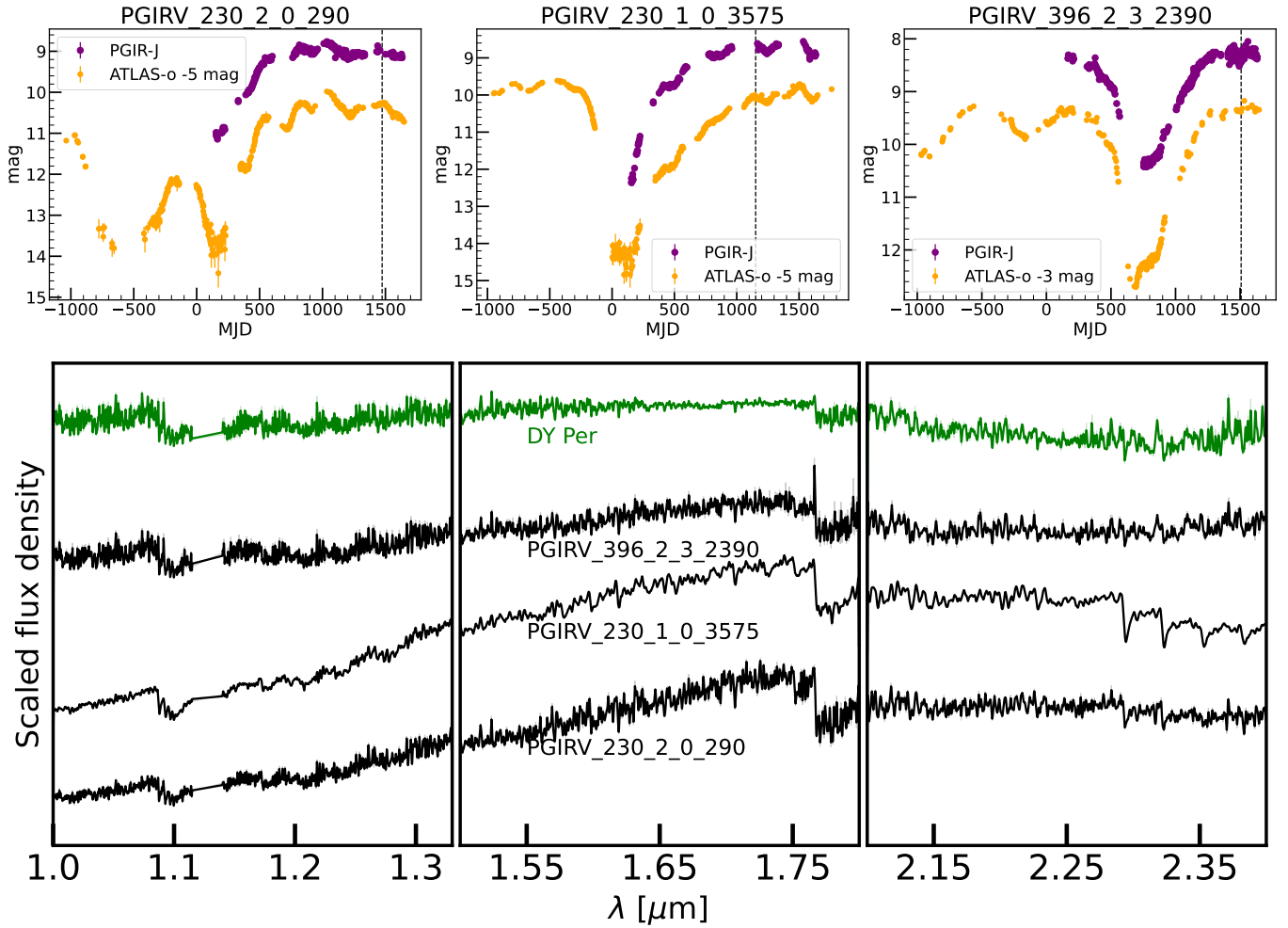


Figure 5. NIR spectra of new RCB stars (continued from Fig. 4)

**Table 3.** RCB and DY Per stars identified/confirmed from our NIR census (continued in Table 4)

Name	ToI-ID/ PGIR Name	RA deg	Dec deg	NIR spec. class	Comments
WISE J174317.52-182402.4	185	265.82303	-18.40068	RCB	a
WISE J175317.73-194632.5	195	268.32389	-19.77572	RCB	
WISE J182501.85-230803.9	226	276.25772	-23.13444	RCB	b
WISE J182801.05-100916.7	230	277.00438	-10.15464	RCB	
WISE J183213.53+050454.5	235	278.05638	5.08181	RCB	
WISE J184102.48-004136.3	248	280.26034	-0.69344	RCB	
WISE J190918.81+030531.2	270	287.32838	3.09201	RCB	
WISE J175725.03-230426.4	1245	269.35429	-23.07402	RCB	
WISE J180021.11-232202.9	1248	270.08797	-23.36749	RCB	
WISE J203825.90+514140.7	1420	309.60795	51.69464	RCB	
WISE J221558.89+422246.2	1444	333.99538	42.37950	RCB	
WISE J223517.61+593812.7	1446	338.82341	59.63688	RCB	
WISE J202514.28+472731.5	2938	306.30950	47.45877	RCB	
WISE J181706.84-235751.3	4108	274.27851	-23.96426	RCB	h
WISE J175136.80-220630.6	194	267.90335	-22.10852	RCB	c
WISE J180313.12-251330.1	207	270.80467	-25.22505	RCB	c
WISE J183631.25-205915.1	4117	279.13024	-20.98755	RCB	c
WISE J172044.89-315031.7	164	260.18707	-31.84215	RCB	c, g
WISE J173837.00-281734.5	181	264.65417	-28.29292	RCB	c, g
WISE J190309.89-302037.1	264	285.79123	-30.34365	RCB	c, g
WISE J004822.34+741757.4	6	12.09309	74.29928	RCB	e
WISE J005128.08+645651.7	8	12.86702	64.94770	RCB	e
WISE J175749.76-075314.9	203	269.45737	-7.88750	RCB	d, e
WISE J181836.38-181732.8	222	274.65160	-18.29247	RCB	e
WISE J182010.96-193453.4	223	275.04570	-19.58150	RCB	e
WISE J182235.25-033213.2	225	275.64690	-3.53701	RCB	e
WISE J184158.40-054819.2	249	280.49336	-5.80535	RCB	d, e
WISE J190813.12+042154.1	268	287.05469	4.36503	RCB	e
WISE J191243.06+055313.1	274	288.17945	5.88698	RCB	e
WISE J192348.98+161433.7	281	290.95410	16.24270	RCB	e
WISE J194218.38-203247.5	290	295.57660	-20.54654	RCB	d, e
WISE J170552.81-163416.5	1213	256.47005	-16.57125	RCB	e
WISE J173737.07-072828.1	1225	264.40446	-7.47449	RCB	e
WISE J185726.40+134909.4	1309	284.36004	13.81930	RCB	e
WISE J172951.80-101715.9	174	262.46586	-10.28778	RCB	d
WISE J174645.90-250314.1	188	266.69128	-25.05392	RCB	d
WISE J175107.12-242357.3	193	267.77967	-24.39927	RCB	d
WISE J181538.25-203845.7	220	273.90938	-20.64604	RCB	d
WISE J182943.83-190246.2	231	277.43263	-19.04617	RCB	d
WISE J185525.52-025145.7	257	283.85636	-2.86271	RCB	d
WISE J173819.81-203632.1	1227	264.58255	-20.60893	RCB	d
WISE J181252.50-233304.4	2645	273.21875	-23.55124	RCB	d
WISE J182723.38-200830.1	1269	276.84744	-20.14172	RCB	d
WISE J180550.49-151301.7	209	271.46038	-15.21714	RCB	d
WISE J175558.51-164744.3	197	268.99382	-16.79565	RCB	d
WISE J175749.98-182522.8	204	269.45827	-18.42300	RCB	d
WISE J175031.70-233945.7	191	267.63210	-23.66270	RCB	d

*a* : Listed as a RCB candidate based on the *Gaia* lightcurve by Eyer et al. (2023). *b* : Listed as a RCB candidate based on its lightcurve by Maíz Apellániz et al. (2023). *c* : Listed as strong RCB candidates by Tisserand et al. (2020), *d* : Classified as RCB stars from optical spectra by Tisserand et al. (2020), *e* : Also presented in our previous pilot NIR spectroscopic paper Karambelkar et al. (2021), *f* : Flagged as a possible RCB star on AAVSO by Gabriel Murakawski. *g* : Targets with declination  $< -28^\circ$  that were observed as they were listed as strong RCB candidates, *h* : Listed as RCB star V2331 Sgr in Crawford et al. (2023).



**Figure 6.** *Top:* Lightcurves of new DYPer type stars. Purple dots show the PGIR data and orange dots show the shifted ATLAS-o band data. *Bottom:* NIR spectra of the new DYPer type stars (black) and DY Per itself (green). The spectra of the new stars closely resemble that of DY Per and N-type carbon stars.

**Table 4.** RCB and DY Per stars identified/confirmed from our NIR census (continued from Table 3)

Name	ToI-ID/ PGIR Name	RA deg	Dec deg	NIR spec. class	Comments
WISE J184246.26-125414.7	250	280.69277	-12.90409	RCB	d
WISE J174138.87-161546.4	182	265.41199	-16.26291	RCB	d
WISE J183649.54-113420.7	240	279.20645	-11.57244	RCB	d
IRAS 19437+2812	PGIRV_526_1_0_2033	296.4334005	28.33476509	RCB	
MGAB-V209	PGIRV_663_2_3_2970	288.3546954	17.61718824	RCB	f
C*2610		278.80827	-15.60382	RCB	a
IRAS 21210+4922	PGIRV_230_2_0_290	320.699761	49.58775202	DY Per	
BC 279	PGIRV_230_1_0_3575	316.0404598	51.96017409	DY Per	
NC50_6	PGIRV_396_2_3_2390	300.5364042	36.46534761	DY Per	

*a* : Listed as a RCB candidate based on the *Gaia* lightcurve by Eyer et al. (2023). *b* : Listed as a RCB candidate based on its lightcurve by Maíz Apellániz et al. (2023). *c* : Listed as strong RCB candidates by Tisserand et al. (2020), *d*: Classified as RCB stars from optical spectra by Tisserand et al. (2020), *e*: Also presented in our previous pilot NIR spectroscopic paper Karambelkar et al. (2021), *f*: Flagged as a possible RCB star on AAVSO by Gabriel Murakawski.

#### 4.2.2. New DY Per type stars

DY Per type stars are thought to be a colder sub-class of RCB stars (with  $T_{\text{eff}} \approx 3500\text{K}$ ), marked by shallower and more symmetric declines in their lightcurves than RCB stars (Alcock et al. 2001). From our PGIR lightcurve-selected candidates, we identified three stars that show lightcurves and spectra resembling DY Per type stars. Fig. 6 show the PGIR-J band and ATLAS-o band lightcurves of these stars. For two of them, the PGIR lightcurves sample only the rise out of the decline, but the longer baseline ATLAS lightcurves show DY Per-like variations. The NIR spectra of these stars very closely resemble N-type carbon star templates from the IRTF spectral library (Rayner et al. 2003). All three stars have NIR colors similar to known DY Per type stars (Tisserand et al. 2013). We classify these three as new Galactic DY Per type stars.

#### 4.3. PGIR lightcurves of known carbon-stars

##### 4.3.1. New RCB star

Using the PGIR lightcurves of stars classified as “carbon-stars” on Simbad, we identified one previously unknown RCB candidate – C\*2610 – that shows large-amplitude RCB-like declines in its lightcurve. We classify it as an RCB star based on its NIR spectrum which resembles RCB stars undergoing declines. This source was also listed as a possible RCB star based on its *Gaia* lightcurve by Eyer et al. (2023), and appears in the carbon-star catalogs of Stephenson (1973) and Alksnis et al. (2001). This star is listed in Table 3 and its PGIR lightcurve and NIR spectra are included in Fig. 3 and 5 respectively.

##### 4.3.2. New DY Per candidates

From the Simbad “carbon-star” lightcurves, we identify 15 stars that show variations resembling DY Per. We list these stars as candidate DY Per type stars in Table 8, as we do not have spectroscopic observations for them. These PGIR lightcurves of these stars are shown in Fig. 12.

## 5. DISCUSSION

### 5.1. Total number of Galactic RCB stars

#### 5.1.1. Total RCB stars in the T20 catalog

First, we determine the total number of RCB stars in the T20 catalog. We identified a total of 50 RCB stars (see Sec. 4.1 and Fig. 1). As noted earlier, 3 of these belong to Priority G ( $\text{decl.} < -28^\circ$ ) which is not amongst our prioritized categories, so we do not use these to determine the total number. The remaining 47 RCB stars come from our systematic followup of prioritized categories highlighted in Fig. 1.

For lightcurve Priority A (see Fig. 1), we observed all 176 candidates and identified 33 RCB stars. For lightcurve priorities (lc-pri) B, C and D, we only observed the color-priorities (col-pri) 1-a, 2-a and 3-a. We use these observations to estimate the numbers in col-pri 1-b, 2-b and 3-b.

First, in col-pri 1-a and lc-pri B+C+D, we observed all 104 candidates and identified 12 RCB stars. For col-pri 1-b and lc-pri B+C+D, we observed 11 out of 36 candidates and identified no RCB stars, but 1 strong RCB candidate. Scaling to the total number of candidates in this category, we expect no more than  $\approx 3$  RCB stars in 1-b. The efficiency is expected to be lower in 1-b than 1-a as 1-b is more contaminated by RV-Tauri stars. For col-pri 1-c and lc-pri B+C+D, we expect the

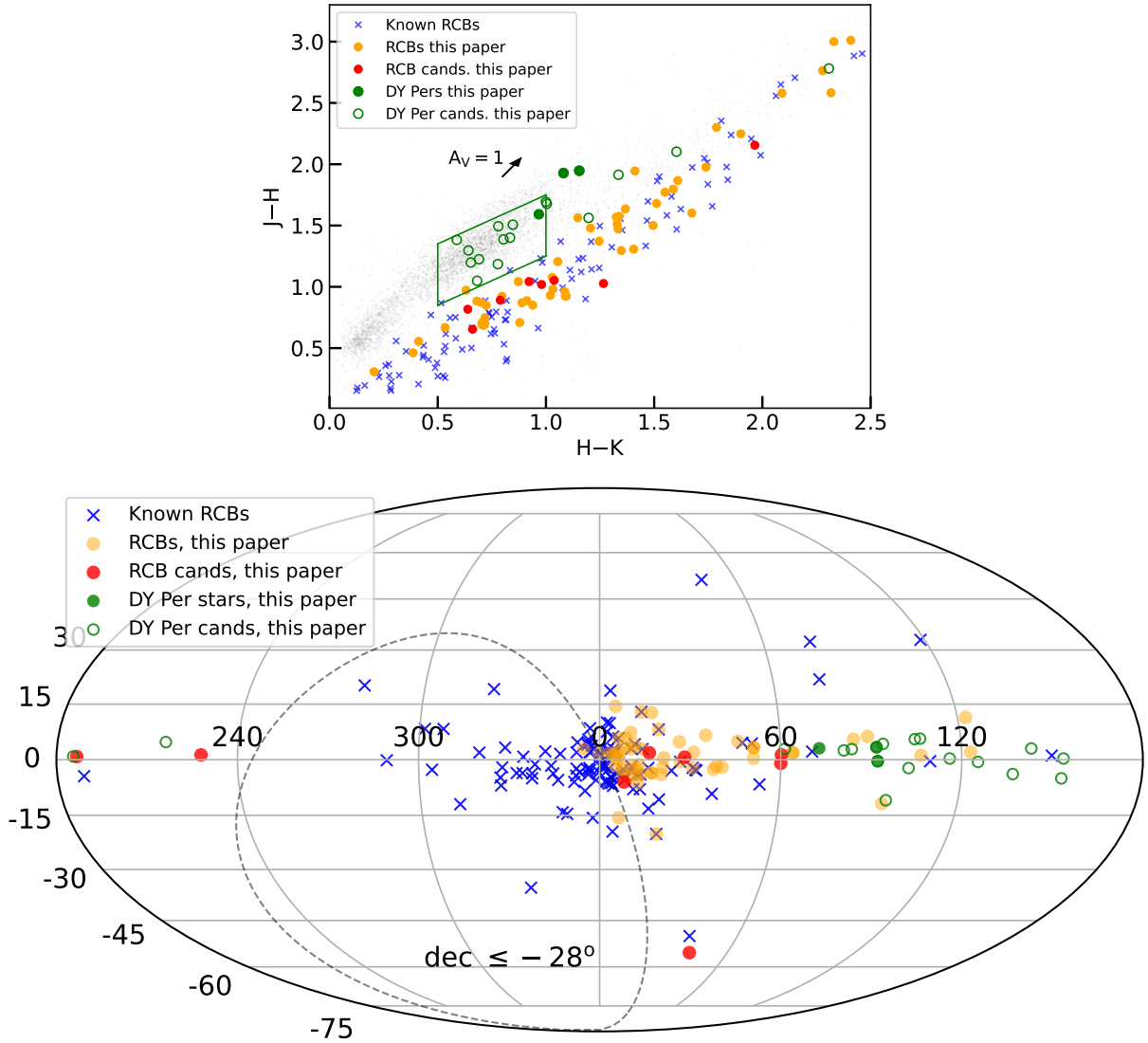


**Figure 7.** *Top:* 2MASS color-color diagram for known RCB stars (blue crosses), new RCB stars (orange dots), new RCB candidates (red dots), new DY Per type stars (green solid dots) and new DY Per candidates (hollow green circles). The green box marks the DY Per-selection region from Tisserand et al. (2013), and the black arrow indicates the direction of interstellar extinction of  $A_V = 1$  mag. The DY Per type stars follow a distinct trend than the RCB stars. *Bottom:* Galactic distribution of RCB and DY Per type stars. Most RCB stars are located towards the center of the Milky Way, consistent with a bulge population, while most DY Per type stars are located at high Galactic longitudes, indicative of a disk population.

contamination of LPVs to be much higher than 1-a+1-b. Based on the estimate in Karambelkar et al. (2021), we expect 1-c to have 5 times more LPVs and 10 times fewer RCBs than 1-a and 1-b combined. Therefore, for the ambiguous and non-detection lightcurves (lc-pri B and D) in 1-c, we estimate the RCB-occurrence rate to be 50 times lower than 1-a and 1-b. For flat lightcurves (lc-pri C), we assume the same RCB-occurrence rate in 1-c as in 1-a + 1-b. This gives a total expected number of 3 RCB stars in 1-c.

Second, in col-pri 2-a and lc-pri B+C+D, we observed 50 candidates and identified 1 RCB star. Assuming this

RCB-occurrence rate, we expect 1 RCB star in col-pri 2-a and 4 RCB stars in col-pri 2-b.

Finally, for col-pri 3-a and lc-pri B+C+D, we observed 44 out of 45 candidates and identified 1 RCB star. The low efficiency is expected, as these are the brightest targets in group 3, which coincide with stars with a classification listed on Simbad. Category 3-b groups the candidates with at least one upper limit in the 4 WISE bands. Optimistically, we choose an RCB efficiency of  $\approx 20\%$  for this category (following Tisserand et al. 2020), we estimate another 29 RCB stars from col-pri 3-b and lc-pri B+C+D to account for a population of highly dust

**Table 5.** Total number of RCB stars identified in the T20 catalog for different color and lightcurve priorities. \* marks categories which were not covered in our spectroscopic followup. The numbers in these categories were determined as described in Sec. 5.1.1

col-pri	lc-pri	lc-pri
	A	B+C+D
1-a	20	12
1-b	2	3*
1-c	9	3*
2-a	0	1
2-b	1	4*
3-a	1	1
3-b	0	29*

enshrouded RCB stars. Table 5 shows a summary of number of RCB stars in each of the categories discussed above.

In total, we estimate there are  $\approx 86$  RCB stars (95% confidence interval 60 – 150) out of the 1215 candidates from the T20 catalog with northern declinations ( $\delta > -28^\circ$ ). Accounting for southern candidates, 85% completeness and adding the 77 known RCB stars gives a total of  $86 \times (100/85) \times (2194/1215) + 77 = 260$  (95% confidence interval 200 – 390). Including the 8 strong RCB candidates gives a total of 280 (95% CI 210 – 400) RCB stars in the full T20 catalog.

#### 5.1.2. Total Galactic RCB stars

We now discuss possible biases associated with our search, and correct for them to determine the total number of Galactic RCB stars. First, as noted in Tisserand et al. (2020), the detection efficiency of the catalog drops within a few degrees of the Galactic center and along the Galactic plane at low Galactic latitude due to high interstellar extinction. We used the white-dwarf binary population synthesis model from Lamberts et al. (2019) to estimate the number of RCB stars within this region. From the simulated white-dwarf binaries, we calculate the number of He-CO WD binaries that are within 2 degrees of the Galactic center, or within  $1^\circ$  of the Galactic plane. We find that  $\approx 20\%$  of all He-CO WD binaries lie within this region. Assuming that RCB stars follow a similar distribution, we estimate that there are  $\approx 70$  RCB stars within this region that are missed by our search. We derive a similar number using star counts generated from the Besancon model of the Milky Way (Czekaj et al. 2014). Future high-spatial resolution observations (e.g. with the *Roman* space telescope) can accurately measure the number of RCB stars in this highly crowded region. Our rough estimate suggests a total of

$\approx 350$  (C.I. 250 – 500) RCB stars in the Milky Way. This estimate agrees well with the estimate of 300 – 500 from Tisserand et al. (2020).

Second, the T20 catalog is expected to contain 85% of RCB stars based on previously known RCB stars, that come from a non-homogenous sample. We use our color-independent PGIR lightcurve-based search to test this 85% completeness estimate. After applying our lightcurve selection criteria ( $\eta < 0.5$  and  $\text{ptp} > 2$ ) on lightcurves in the PGIR database, we recover a total of 24 RCB stars. 22 of them are either previously known RCB stars or present in the T20 catalog. Only 2 RCBs are previously unknown and are not present in the catalog. Other than these 2, we do not find any RCBs in the lightcurve selected candidates. This suggests that the 85% completeness estimate of the T20 catalog is reasonable. We note that the completeness of the PGIR lightcurve database is not well quantified, but it is unlikely that we are missing a substantial population of RCB stars.

Finally, we quantify the efficiency of PGIR in detecting RCB stars. We created a simulated distribution of 10000 RCB stars in the Milky Way assuming that the distribution traces the Galactic stellar mass. We use the SED of the prototype star R CrB together with interstellar extinction values from Green et al. (2019) to predict the expected distribution of the brightness of RCB stars visible from the northern hemisphere ( $\delta > -28^\circ$ ). Fig. 8 shows the distribution of apparent magnitudes of the simulated RCB stars in the *J* and optical *g* and *r* bands. We find that PGIR with a limiting magnitude  $m_{\text{lim}} \approx 13 - 15$  mag is sensitive enough to detect  $> 90\%$  of RCB stars at maximum light. PGIR will thus detect almost all RCB stars in the northern hemisphere that brightened to maximum light over its five year baseline. Declines longer than 5 years are seen in known RCB stars, such as the historic 10-year dimming of R CrB itself in 2007. Examining declines in all known RCB stars using long-baseline AAVSO lightcurves, Crawford et al. (2024, in prep.) finds that 30 out of 1039 (3%) declines are longer than 5 years, and additionally that the coldest RCB stars are prone to both more frequent declines and spending more than 80% of observed time in decline phase. These cool stars occasionally not show any brightness variations and would thus not be identified as large amplitude variables. However, they would still pass the lightcurve-independent color-selection criteria. Specifically, as mentioned in Sec. 5.1.1, col-pri 3-b accounts for highly dust-enshrouded cold RCB stars that spend most of their time in a dust-enshrouded phase and do not rise to maximum light. Interestingly, Fig. 8 shows that PGIR has the same RCB-detection efficiency as an

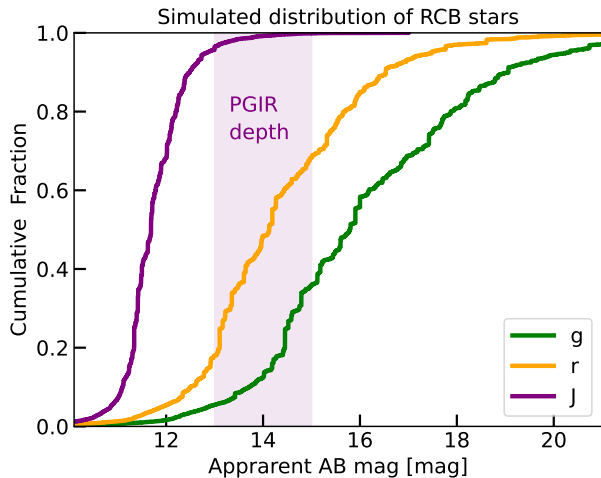


**Figure 8.** Distribution of the apparent magnitudes of simulated Galactic RCB stars at maximum light, that are visible from the northern hemisphere. The shaded purple region shows the typical range of PGIR limiting magnitudes (which varies depending on the extent of confusion). PGIR is sensitive enough to detect  $> 90\%$  of RCB stars at maximum light. PGIR can detect almost all RCB stars that brightened to maximum light in the last five years. PGIR has the same RCB-detection efficiency as an optical survey with a much deeper limiting magnitude ( $\approx 20$  mag) – illustrating the advantages of a NIR search for dusty RCB stars.

optical survey with a much deeper limiting magnitude ( $m_{\text{lim}} \approx 20$  mag, e.g. ZTF) – illustrating the advantages of a NIR search at finding dusty RCB stars in dusty regions of the Milky Way.

To summarize, we determine that there are a total of 350 RCB stars in the Milky Way (C.I. 250–500). Despite the biases associated with our search listed here, the total number of Galactic RCB stars is unlikely to be substantially larger than this estimate.

### 5.1.3. Comparisons with the rate of He-CO WD mergers

Using our derived number of 350 (C.I. 250–500) Galactic RCB stars and assuming typical RCB lifetimes of  $1 - 3 \times 10^5$  yr (Schwab 2019; Crawford et al. 2020; Wong & Bildsten 2024), the formation rate of RCB stars, in the Milky Way is between  $0.8 - 5 \times 10^{-3} \text{ yr}^{-1}$ . This is consistent with observational and theoretical estimates of the He-CO WD merger rate. Using observations of low-mass WD binaries in the Milky Way disk from the ELM survey, Brown et al. (2020) estimate a lower limit of  $2 \times 10^{-3} \text{ yr}^{-1}$  on the rate of He-CO WD mergers. Using binary population synthesis models, Karakas et al. (2015) estimate a He-CO WD merger rate of  $\sim 1.8 \times 10^{-3} \text{ yr}^{-1}$ .

The population of RCB stars can provide useful information for future gravitational wave missions like LISA.

Recently, Lamberts et al. (2019) found that close He-CO double white dwarfs (DWDs) will constitute the majority of sources detectable with LISA, and predicted over 5000 He-CO DWD resolvable over a 4 year baseline. As RCB stars are remnants of He-CO WD mergers, they serve as an independent probe of these predictions. We start with the simulated short-period (lower than few hours) He-CO WD binaries from Lamberts et al. (2019) and evolve them assuming gravitational wave radiation dominates the binary evolution, and find a He-CO WD merger rate of  $\approx 1 \times 10^{-3} \text{ yr}^{-1}$ . Assuming RCB-lifetimes as above, this corresponds to an expected number of 100–300 RCB stars in the Milky Way. It is encouraging that this estimate is broadly consistent with the observed number of RCB stars despite simplified assumptions about WD binary evolution. More detailed simulations that account for different RCB-lifetimes, RCB progenitor-mass ranges and WD-merger physics such as mass transfer can provide observationally-grounded predictions for the dominant population of DWDs that should be detectable with LISA.

Missing from this picture are dLHdC stars. As noted in Tisserand et al. (2022), there could be as many, if not more, dLHdC stars in the Milky Way as RCB stars. There are several indications that the population of WDs that merge to form RCB stars have distinct properties from those that form dLHdC stars (Karambelkar et al. 2022; Tisserand et al. 2022; Crawford et al. 2022). The lower luminosities and oxygen isotope ratios suggest that dLHdC stars could come from lower mass mergers than RCB stars. From BPS simulations, Tisserand et al. (2022) find that the distribution of total masses of WD merger remnants is bimodal, with the higher end ( $\approx 0.9 M_{\odot}$ ) coming from hybrid-CO + CO WD mergers. If RCB stars form preferentially from these higher mass mergers, the RCB formation rate derived here corresponds to the rate of hybrid-CO + CO WD mergers rather than the full rate of He-CO WD mergers. Accurate mass measurements of RCB and dLHdC stars will help understand the implications of the RCB formation rate on the rate of WD mergers.

### 5.2. Pulsation periods

At maximum light, some RCB stars are known to pulsate with periods between 40-100 days and amplitudes of a few tenths of a magnitude (Lawson & Cottrell 1997; Alcock et al. 2001; Percy 2023). These pulsations can be fairly irregular – the star can exhibit multiple pulsation modes or undergo changes in the dominant period (e.g. R CrB has shown pulsations with periods of 33, 44, 52 and 60 days (Lawson & Kilkenny 1996)). Initially, these semi-regular or irregular pulsations were



suggested to originate from the strange-mode instability in non-adiabatic and radiation-pressure dominated envelopes (Saio 2008; Gautschy 2023). Recently, Wong & Bildsten (2024) modeled the RCB-dLHdC pulsations as solar-like oscillations excited by convection in a helium-rich envelope. They find that the frequencies with maximum power ( $\nu_{\max}$ ) for such oscillations matches the observed range of periods in RCBs and dLHdCs. These models show that the pulsation periods can be used as diagnostics of the mass of the stars, with lower periods generally indicative of lower masses.

We examined the *J*-band PGIR light curves of the RCB stars presented in this paper, 70 previously known RCB stars to search for maximum-light periodic variations. We identified windows in the light curves that show periodic variations, and derived the periods using the Lomb-Scargle implementation in the `python` package `gatspy`. We derive pulsation periods for 16 RCB. To derive errorbars on the periods, for each star, we used the measured brightness and uncertainties to generate 100 simulations of the lightcurve assuming a normal distribution and measured the periods for each lightcurve. The median periods and standard deviations are listed in Table 6. The periods typically lie between 30–100 days. Periods of some of these stars have been previously reported based on optical photometry – SU Tau ( $\sim 40$  d, Lawson et al. 1990), FH Sct ( $\sim 47$  d, Percy 2023), R CrB (multiple periods ranging from  $\sim 35 - 60$  d Lawson & Kilkenny 1996), C105 ( $\sim 40$  d, Tisserand et al. 2022). The PGIR periods of these stars are consistent with those reported previously.

In addition to the PGIR lightcurves, we also examined lightcurves of RCB and dLHdC stars from the Transiting Exoplanet Satellite Survey (*TESS*, Ricker et al. 2015) to search for short-timescale variability from them. We downloaded calibrated, short-cadence *TESS* lightcurves from the Quicklook Pipeline (QLP) for known RCB and dLHdC stars from the Mikulski Archive for Space Telescopes<sup>3</sup> using `astroquery`. We examined simple aperture photometry (SAP) lightcurves for each star and removed lightcurves which have bad photometric flags, large photometric scatter and rapid increases or decreases of flux that are likely not astrophysical. Additionally, we also use the `python` package `lightkurve` to download the *TESS* target pixel files and extract aperture photometry at the locations of known RCB and dLHdC stars. We find that the QLP lightcurves agree well with those extracted using `lightkurve`, where available. We use the DREAMS-RCB monitoring website to determine the

**Table 6.** Pulsation periods using PGIR lightcurves

Name	PGIR Period days
ASAS-RCB-8	$27 \pm 6$
ASAS-RCB-18	$41 \pm 8$
FH Sct	$44 \pm 11$
NSV 11154	$70 \pm 20, 45 \pm 5$
R CrB	$67 \pm 10$
SU Tau	$58 \pm 10$
SV Sge	$53 \pm 10$
UV Cas	$41 \pm 10$
V532 Oph	$38 \pm 10$
WISE J005128.09+645651.73	$34 \pm 6$
WISE J182801.05-100916.71	$170 \pm 10$
WISE J181252.50-233304.47	$48 \pm 15$
WISE J172951.80-101715.9	$60 \pm 19$
WISE J183649.54-113420.7	$59 \pm 9$
Z Umi	$42 \pm 10$
C105	$33 \pm 10$

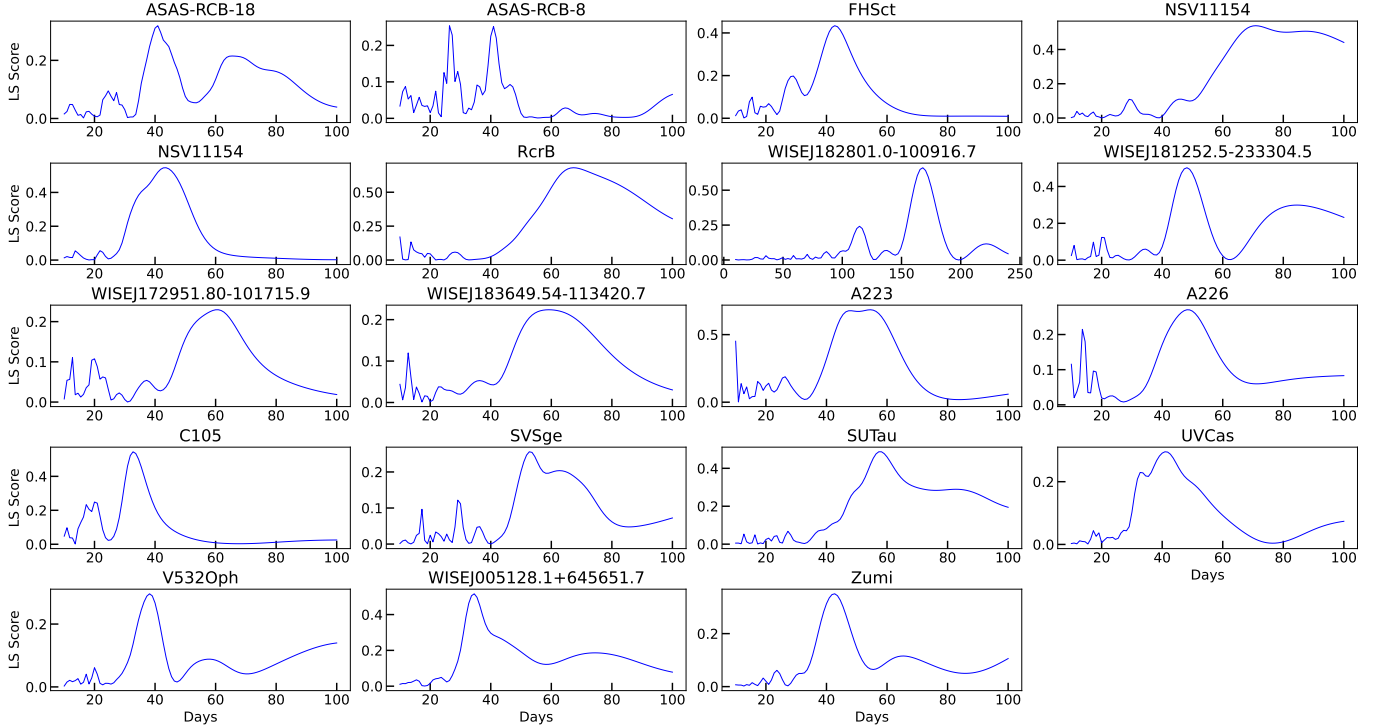
photometric phase of the RCB stars at the time of *TESS* observations and use only those lightcurves that were observed at maximum light. We are then left with 6 RCB stars and 6 dLHdC stars. The *TESS* lightcurves have cadences of 10 and 30 minutes, and a baseline of  $\approx 22 - 27$  days per sector. Some stars were observed in multiple sectors. As it is challenging to stitch data from different sectors together if they are not observed continuously, we analyze the different sectors individually.

Figure 10 shows the median-normalized *TESS* lightcurves of six RCB and six dLHdC stars. The *TESS* lightcurves show that both RCB and dLHdC stars do not show variability at very short ( $< 1$  day) timescales. Interestingly, these high-cadence lightcurves show that dLHdC stars generally exhibit variability on timescales shorter than RCB stars. In the picture that dLHdC stars have lower masses than RCB stars, they are expected to have smaller pulsation periods than RCB stars (Wong & Bildsten 2024). The differences seen in the *TESS* lightcurves of RCBs and dLHdCs may therefore point towards the different masses of this class of objects, as suggested in Tisserand et al. (2022); Karambelkar et al. (2022). Studying the variations of a larger sample of dLHdC and RCB stars will provide an important clue towards identifying their masses and possible differences.

### 5.3. Radial velocities

We use our NIR spectra to derive the radial velocities (RVs) of the newly identified RCB stars. We correct the spectra for barycentric motion, examine them to iden-

<sup>3</sup> <https://mast.stsci.edu>



**Figure 9.** Periodograms of RCB and dLHdC stars using PGIR lightcurves reported in Table 6

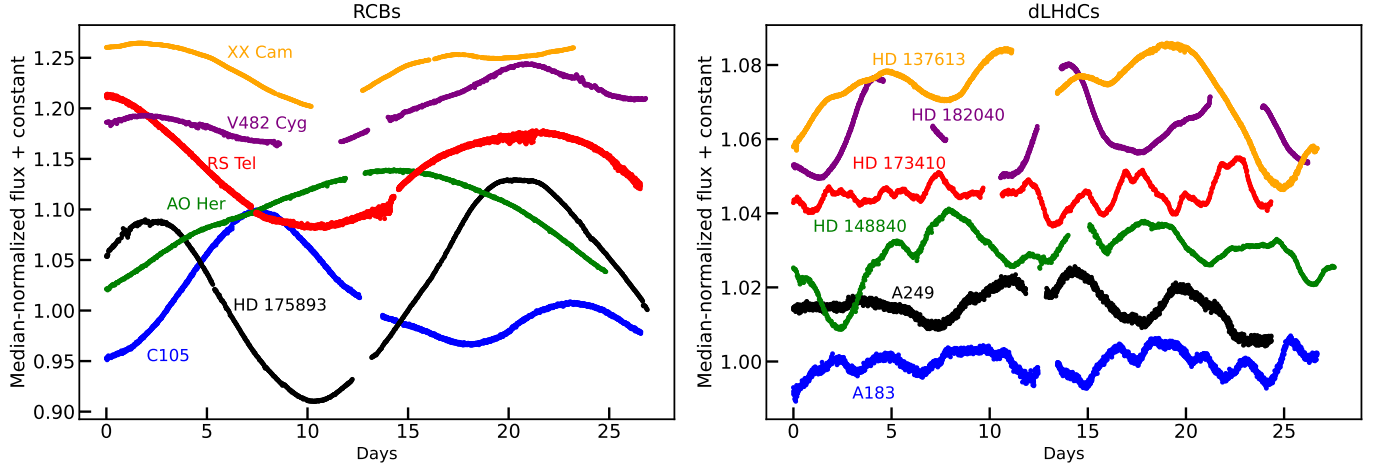


**Figure 10.** *Top* : Examples of *TESS* lightcurves of RCB stars (*left*) and dLHdC stars (*right*). *Bottom* : Lomb-Scargle periodograms of RCB stars (*left*) and dLHdC stars (*right*). dLHdC stars in general show variability on timescales shorter than RCB stars. A possible explanation is that dLHdC stars have lower mass than RCB stars.

tify strong carbon absorption lines, and fit a gaussian profile to derive the line centers. We then compare the line-centers to rest-wavelengths (taken from NIST) to measure the RVs. For each spectrum, we determined the statistical uncertainty on the RV using by calculating the standard deviation of the velocities measured from each carbon line examined. These uncertainties are small (typically  $< 5 \text{ km s}^{-1}$ ). To determine the sys-

tematic uncertainty on how precisely line centroids can be measured due to instrumental resolution, we use the sky-emission lines in our spectra. The dispersion on the sky line centroids is  $20 \text{ km s}^{-1}$  (approx. a third of a pixel). We add the statistical and systematic uncertainties in quadrature and report those as uncertainties on the RVs in Table 7.

**Table 7.** Radial velocities derived from C absorption lines in the NIR spectra. Sources marked with \* denote revised values from the ones reported previously in Karambelkar et al. (2021)

Name	Radial velocity km/s
WISE-ToI-164	$-27 \pm 20$
WISE-ToI-174	$-96 \pm 25$
WISE-ToI-185	$-68 \pm 20$
WISE-ToI-188	$-9 \pm 20$
WISE-ToI-193	$-122 \pm 20$
WISE-ToI-194	$120 \pm 20$
WISE-ToI-207	$-40 \pm 20$
WISE-ToI-220	$-101 \pm 20$
WISE-ToI-226	$-146 \pm 20$
WISE-ToI-231	$7 \pm 25$
WISE-ToI-248	$-44 \pm 25$
WISE-ToI-257	$27 \pm 20$
WISE-ToI-264	$120 \pm 20$
WISE-ToI-270	$69 \pm 22$
WISE-ToI-323	$-119 \pm 20$
WISE-ToI-1227	$-43 \pm 20$
WISE-ToI-1241	$-74 \pm 20$
WISE-ToI-1245	$3 \pm 20$
WISE-ToI-2645	$40 \pm 20$
WISE-ToI-2938	$-39 \pm 20$
WISE-ToI-4108	$173 \pm 20$
WISE-ToI-4117	$18 \pm 20$
*AO Her	$-524 \pm 20$
*ASAS-RCB-21	$20 \pm 20$
*NSV 11154	$-326 \pm 22$
*V391 Sct	$-36 \pm 25$
*WISE-ToI-249 <sup>a</sup>	$81 \pm 20$
*WISE-ToI-203 <sup>a</sup>	$-18 \pm 20$
*WISE-ToI-290 <sup>a</sup>	no C lines
*WISE-ToI-6	$-101 \pm 20$
*WISE-ToI-223	$37 \pm 20$
*WISE-ToI-268	$95 \pm 20$
*WISE-ToI-274	$-36 \pm 20$
*WISE-ToI-1309	$-13 \pm 20$
*WISE-ToI-281	no C lines
*WISE-ToI-1213	no C lines

<sup>a</sup> : The stars WISE-ToI-203, 249 and 290 are listed as WISE-J17+, WISE-J18+ and WISE-J19+ in Karambelkar et al. (2021).

We also note an error in the RVs reported in our previous paper (Karambelkar et al. 2021) – the signs of the values in Table 3 there should be flipped. Additionally, we note that the previous values were measured by cross-correlating the entire spectrum with synthetic RCB spectra, while here, we measure the values using only strong carbon absorption lines. We find that the RVs measured using carbon lines are more reliable, as the spectral features in the synthetic models are highly dependent on the assumed elemental abundances of the RCB star. Indeed, we find that the RVs reported here agree better with those reported by other sources wherever available (e.g. *Gaia*, see Tisserand et al. 2024a). Table 7 also lists the revised RVs for these stars. Most RCB stars in Table 7 have low RVs ( $\leq 50 \text{ km s}^{-1}$ ), consistent with other RCB stars with RV measurements (Tisserand et al. 2024a). AO Her and NSV 11154 have very high RVs, and are located towards the Galactic halo. The RVs reported here will be useful in constructing the 3D-distribution of Galactic RCB stars (similar to Tisserand et al. 2024a).

#### 5.4. Are RCB and DY Per type stars related?

First, we note that neither DY Per, nor the three spectroscopically confirmed DY Per type stars show the He I ( $\lambda 10830$ ) line that is ubiquitous in RCB stars. In RCB stars, this line is collisionally excited in high velocity ( $\approx 400 \text{ km s}^{-1}$ ) He-rich dust-driven winds (Clayton et al. 2013; Karambelkar et al. 2021). DY Per type stars resemble classical carbon-stars in this aspect. However, even in the cold-RCB picture, the absence of this line can possibly be explained by the low-luminosity of DY Per type stars compared to RCB stars. As DY Per type stars are  $\approx 10$  times dimmer than RCBs, the radiation pressure can accelerate only low velocity winds ( $\approx 40 \text{ km s}^{-1}$ , assuming ), which is not sufficient to excite the helium atoms to the lower energy level of the He I transition.

Second, Fig. 7 (bottom panel) shows the Galactic distribution of the RCB and DY Per type stars identified in this paper together with known RCB and DY Per type stars. Most RCB stars lie towards the Galactic center, with a small number at higher Galactic latitudes suggestive of a small halo population. In contrast, the DY Per type stars and candidates lie at high Galactic longitudes, suggesting that they are part of a disk population. This is consistent with the findings of Tisserand et al. (2024a) who studied the distribution of RCB and DY Per type stars using *Gaia* DR3. The top panel of Fig. 12 shows the NIR color-color diagram for RCB and DY Per type stars. We find that the new DY Per type stars and DY Per candidates occupy a distinct region in this diagram from RCB stars and have colors similar to

classical carbon stars, consistent with Tisserand et al. (2013).

We also note that the new DY Per type stars and candidates show some diversity in their lightcurves. We plot longer baseline ATLAS-o band lightcurves of the DY Per type stars and candidates in Fig. 6 and Fig. 12. Some stars (e.g. PGIRV\_396, PGIRV\_230\_1\_0\_3575, NIKC 2-77, V\*FL Per, Fuen C 157) show well-defined brightness-declines that are clearly distinguishable from other small-amplitude variations, while some stars (e.g. IRAS 04193+, IRAS 07113+, C\*2905, Fig. 12) generally show large-amplitude erratic variations without well-defined declines. The lightcurves of some stars such as PGIRV\_230\_2\_0\_290 (Fig. 6), C2905 and ATO J308.8118 (Fig. 12) show large-amplitude pulsations that are seen in carbon stars. The stars V2060 Cyg, KISO C1-139, IRAS22137+ (Fig. 12) show declines at periodic intervals. Based on the lightcurves of classical carbon stars in the LMC, (Soszyński et al. 2009) suggest that DY Per variability is part of the continuum of carbon-star variability. Spectroscopic observations of the different classes of DY Per candidates will help understand which, if any, of these stars show RCB-like elemental abundances (esp.  $^{18}\text{O}$ ).

## 6. SUMMARY AND WAY FORWARD

In this paper, we presented results from a systematic infrared census for RCB stars in the Milky Way. We selected RCB candidates using NIR  $J$ -band lightcurves from PGIR, mid-IR colors from WISE and obtained medium resolution NIR spectra for them. We identified 53 RCB stars from our candidates. We use this number to estimate the total number of RCB stars in the Milky Way. This has been a longstanding open question - with estimates ranging from a few thousand (Clayton 2012; Han 1998; Alcock et al. 2001) to a few hundred (Tisserand et al. 2020). Our systematic infrared census provides an excellent way to address this question. Using our selection criteria, we estimate that there are a total of  $\approx 350$  RCB stars with a 95% confidence interval of 250 – 500 in the Milky Way. This corresponds to a formation rate of  $0.8 - 5 \times 10^{-3} \text{ yr}^{-1}$ . This is consistent with observational and theoretical estimates of the rate of He-CO WD mergers in the Milky Way. Using binary population synthesis models, the measured RCB-formation rate can be used to draw insights about the population of He-CO WD binaries detectable with future gravitational-wave experiments such as *LISA*. However, in addition to RCB stars, it is important to understand the contribution of the dustless dLHdC stars and colder DY Per type stars to the population of He-CO WD merger remnants.

It is still not clear whether DY Per type stars are colder RCB stars or classical carbon stars. Only 3 Galactic DY Per type stars were known in the Milky Way. In this paper, we identified 3 spectroscopically confirmed and 15 candidate DY Per type stars. The new DY Per type stars and candidates have distinct NIR colors and appear to have a different Galactic distribution than RCB stars. Future analysis of the spectra and long-term photometric variations of these stars will be useful to understand their relation to RCB stars. dLHdC stars have been conclusively associated with He-CO WD merger remnants, but their number is uncertain. As noted in (Tisserand et al. 2022), there could potentially be as many dLHdC stars as RCB stars in the Milky Way. A systematic search for dLHdC stars is required to interpret the number of RCB-dLHdC stars in the context of the He-CO WD merger rate.

The differences between dLHdC and RCB stars have only recently started to be explored. The differences in their luminosities and chemical compositions suggest that dLHdC stars could be less massive than RCB stars (Tisserand et al. 2022; Karambelkar et al. 2022; Crawford et al. 2022). In this picture, we would expect the maximum-light pulsation periods of these stars to differ. The *TESS* lightcurves for six dLHdC and six RCB stars show that dLHdC stars show variations on timescales shorter than RCB stars, consistent with the picture that they have lower masses. Comparing these pulsation data to theoretical models (e.g. Wong & Bildsten 2024; Saio 2008) to estimate their masses will providing useful information towards understand why dLHdCs form dust and RCBs do not.

Finally, we have presented NIR spectra for 44 RCB stars, which can be useful for measuring their elemental abundances. In addition to oxygen isotope ratios (e.g. Karambelkar et al. 2021, 2022), it would be interesting to see if the NIR spectra can be used to solve the longstanding carbon problem in RCBs (Asplund et al. 2000). NIR spectra also probe the helium line, which can be used to study mass-loss in RCB stars (Clayton et al. 2011).

NIR observations are an efficient way to identify and characterize RCB stars. Ongoing and upcoming NIR surveys such as the Wide-field Infrared Transient Explorer (WINTER, Lourie et al. 2020), the Dynamic Red All-sky Monitoring Survey (DREAMS), Cryoscope in Antarctica will help uncover the population of RCB stars in the Milky Way. Future missions such as the *Nancy Grace Roman Space Telescope* will help study the RCB stars in the most crowded central region of the Milky Way. In the optical, the Vera Rubin Observatory has the sensitivity to discover all Galactic RCB

stars in the southern hemisphere, as well as RCB stars in other galaxies out to  $\approx 5$  Mpc, shedding light on the DWD populations of these galaxies.

#### ACKNOWLEDGEMENTS

We thank the anonymous referee for useful suggestions that improved this paper. VK thanks Sunny Wong and Yashvi Sharma for useful discussions. Palomar Gattini-IR (PGIR) is generously funded by Caltech, Australian National University, the Mt Cuba Foundation, the Heising Simons Foundation, the Bi-national Science Foundation. PGIR is a collaborative project among Caltech, Australian National University, University of New South Wales, Columbia University and the Weizmann Institute of Science. MMK acknowledges generous support from the David and Lucille Packard Foundation. J. Soon acknowledges the support of an Australian Government

Research Training Program (RTP) scholarship. Some of the data presented here were obtained with Visiting Astronomer facility at the Infrared Telescope Facility, which is operated by the University of Hawaii under contract 80HQTR19D0030 with the National Aeronautics and Space Administration. This work was supported, in part, by the National Science Foundation through grant PHY-2309135 to the Kavli Institute for Theoretical Physics, and by the Gordon and Betty Moore Foundation through grant GBMF5076.

#### DATA AVAILABILITY

The PGIR *J*-band lightcurves of all 1215 candidates, lightcurves of new RCB stars, NIR spectra of all 453 sources, spectroscopic classifications of all 453 sources (Table 2) and updated priorities of the T20 candidates (Table 1) are publicly available at Zenodo at [10.5281/zenodo.12683154](https://doi.org/10.5281/zenodo.12683154).

### APPENDIX

#### A. CANDIDATE RCB AND DYPER TYPE STARS

Table 8 lists the candidate RCB and DYPer type stars identified in our paper. Fig. 11 shows the lightcurves and spectra of the stars listed as strong RCB candidates. Fig. 12 shows the lightcurves of stars listed as candidate DYPer type stars.

#### B. SOURCE CLASSIFICATIONS

We now discuss classifications of the 453 spectra presented in this paper.

*M stars* – A total of 154 stars have M-type spectra (with broad TiO, VO features) and are thus O-rich AGB stars. We compare the spectra to the IRTF spectral library (Rayner et al. 2009), and determine the best-fit match by performing a least-squares fit. The spectral types of these stars range between M5–M9. Several of these stars show H emission lines – commonly seen in Miras. The strength of these emission lines are known to vary with pulsation phase, and likely originate in pulsation-driven shock heating of the atmospheres (Gray & Corbally 2009).

*Possible symbiotic binaries* – 15 stars show AGB-star-like spectra together with strong emission lines, particularly the He I  $\lambda 10830$  emission line. These stars are possibly symbiotic stars, where the helium line collisionally excited in high velocity winds around the star. 8 stars have spectra similar to M-type stars, while 7 stars have spectra resembling C stars.

*Emission stars* – 32 stars show spectra dominated by emission lines, we classify them as emission stars.

*Dust forming carbon stars* – 42 stars show spectra resembling carbon-stars. 39 of these show a broad absorption feature at  $1.5\mu\text{m}$ . This feature is likely due to HCN + C<sub>2</sub>H<sub>2</sub> and has been previously noted in several carbon stars (Gonneau et al. (2016); Gautschy-Loidl et al. (2004)).

*CO emitters : Possible RV-Tauri or young-stellar objects (YSOs)* – 69 stars show CO emission bands in their spectra. Some of these stars show short-period variations on top of a long-period, large amplitude variation, characteristic of RV-Tauri stars. The remaining stars are likely a combination of RV-Tauri stars and young stellar objects (YSOs) that are known to exhibit CO emission in their spectra.

*H-rich* – 71 stars have spectra with strong absorption lines of hydrogen. These stars are most likely RV-Tauri stars.

*Other* – We identify 2 Wolf-Rayet and 1 post-AGB star. 9 additional stars do not show any obvious strong features in their spectra except some hydrogen lines and no brightness variations, suggesting that they are not RCB stars.

### REFERENCES

- Alcock, C., Allsman, R. A., Alves, D. R., et al. 2001, ApJ, 554, 298
- Alksnis, A., Balklavs, A., Dzervitis, U., et al. 2001, Baltic Astronomy, 10, 1

**Table 8.** Strong RCB and DY Per candidates identified from our NIR census.

Name	ToI-ID/ PGIR Name	RA deg	Dec deg	NIR spec. class	Comments
WISE J060405.01+233304.7	28	91.02088	23.55132	RCB-cand	
WISE J072356.66-124014.0	41	110.98611	-12.67058	RCB-cand	
WISE J182649.64-244532.8	228	276.70684	-24.75912	RCB-cand	
WISE J184016.09-035608.9	245	280.06707	-3.93583	RCB-cand	
WISE J193929.35+244504.0	288	294.87231	24.75113	RCB-cand	
WISE J194739.93+232638.7	293	296.91639	23.44410	RCB-cand	
WISE J222704.54-165948.4	323	336.76892	-16.99678	RCB-cand	
WISE J181400.05-134254.4	1257	273.50025	-13.71511	RCB-cand	
Kiso C1-139		18.13093	62.18622	DY Per-cand	<a href="#">Maehara &amp; Soyano (1987)</a>
NIKC 2-77		55.08234	59.09781	DY Per-cand	<a href="#">Soyano &amp; Maehara (1991)</a>
Fuen C 157		90.42725	24.56634	DY Per-cand	<a href="#">Fuenmayor (1981)</a>
V* FL Per		59.90524	46.46239	DY Per-cand	<a href="#">Lee et al. (1947)</a>
Case 492		330.83864	62.30802	DY Per-cand	<a href="#">Nassau &amp; Blanco (1957)</a>
IRAS 22137+6311		333.83008	63.44256	DY Per-cand	<a href="#">Alksnis et al. (2001)</a>
IRAS 07113-0025		108.47103	-0.51654	DY Per-cand	<a href="#">Alksnis et al. (2001)</a>
V* AR Vul		293.93229	26.55986	DY Per-cand	<a href="#">Nassau &amp; Blanco (1957)</a>
IRAS 04193+4959		65.78151	50.10781	DY Per-cand	<a href="#">Putney (1997)</a>
V* V2060 Cyg		317.43137	54.17533	DY Per-cand	<a href="#">Alksnis et al. (2001)</a>
Kiso C1-24		357.80148	62.38434	DY Per-cand	<a href="#">Maehara &amp; Soyano (1987)</a>
ABC90 cep 7		335.68037	54.59463	DY Per-cand	<a href="#">Alksnis et al. (2001)</a>
Case 749		334.65993	43.77903	DY Per-cand	<a href="#">Blanco (1958)</a>
C* 2905		307.02683	42.91874	DY Per-cand	<a href="#">Stephenson (1973)</a>
ATO J308.8118+45.2629		308.81182	45.26292	DY Per-cand	<a href="#">Alksnis et al. (2001)</a>

All strong RCB candidates are sources from the WISE color-selected catalog of [Tisserand et al. \(2020\)](#). For the DY Per-type candidates, we list the papers that first classified them as carbon stars.

- Asplund, M., Gustafsson, B., Lambert, D. L., & Rao, N. K. 2000, *A&A*, 353, 287
- Bailer-Jones, C. A. L., Rybizki, J., Fouesneau, M., Mantelet, G., & Andrae, R. 2018, *AJ*, 156, 58
- Bellm, E. C., Kulkarni, S. R., Graham, M. J., et al. 2019, *PASP*, 131, 018002
- Bhowmick, A., Pandey, G., Joshi, V., & Ashok, N. M. 2018, *ApJ*, 854, 140
- Blanco, V. M. 1958, *ApJ*, 127, 191
- Brown, W. R., Kilic, M., Kosakowski, A., et al. 2020, *The Astrophysical Journal*, 889, 49
- Clayton, G. C. 1996, *PASP*, 108, 225
- . 2012, *Journal of the American Association of Variable Star Observers (JAAVSO)*, 40, 539
- Clayton, G. C., Geballe, T. R., Herwig, F., Fryer, C., & Asplund, M. 2007, *ApJ*, 662, 1220
- Clayton, G. C., Geballe, T. R., & Zhang, W. 2013, *AJ*, 146, 23
- Clayton, G. C., Herwig, F., Geballe, T. R., et al. 2005, *ApJ*, 623, L141
- Clayton, G. C., Whitney, B. A., Stanford, S. A., & Drilling, J. S. 1992, *ApJ*, 397, 652
- Clayton, G. C., Sugerman, B. E. K., Stanford, S. A., et al. 2011, *ApJ*, 743, 44
- Crawford, C. L., Clayton, G. C., Munson, B., Chatzopoulos, E., & Frank, J. 2020, *MNRAS*, 498, 2912
- Crawford, C. L., Tisserand, P., Clayton, G. C., & Munson, B. 2022, *A&A*, 667, A85
- Crawford, C. L., Tisserand, P., Clayton, G. C., et al. 2023, *MNRAS*, 521, 1674
- Cushing, M. C., Vacca, W. D., & Rayner, J. T. 2004, *PASP*, 116, 362
- Czekaj, M. A., Robin, A. C., Figueras, F., Luri, X., & Haywood, M. 2014, *A&A*, 564, A102
- De, K., Hankins, M. J., Kasliwal, M. M., et al. 2020, *PASP*, 132, 025001
- Eyer, L., Audard, M., Holl, B., et al. 2023, *A&A*, 674, A13
- Feast, M. W. 1997, *MNRAS*, 285, 339

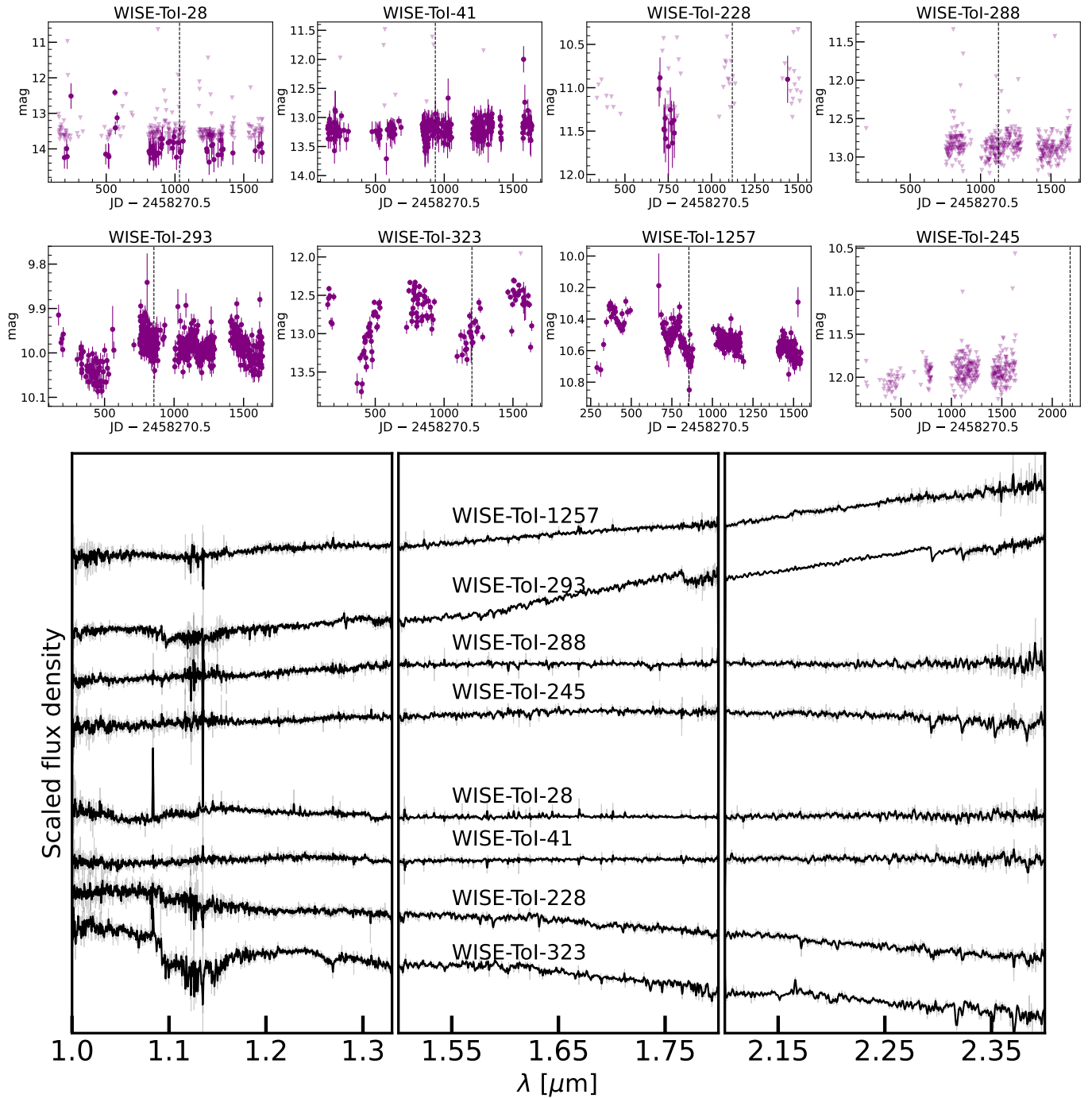


**Figure 11.** NIR spectra of the 8 candidate RCB stars listed in Table 3. The broad absorption feature seen in the spectrum of WISE-ToI-323 from 1.1 – 1.2 $\mu\text{m}$  is likely due to imperfect telluric correction.

Fryer, C. L., & Diehl, S. 2008, in *Astronomical Society of the Pacific Conference Series*, Vol. 391, *Hydrogen-Deficient Stars*, ed. A. Werner & T. Rauch, 335

Fuenmayor, F. J. 1981, *Rev. Mexicana Astron. Astrofis.*, 6, 83

García-Hernández, D. A., Rao, N. K., Lambert, D. L., et al. 2023, *ApJ*, 948, 15

Gautschy, A. 2023, arXiv e-prints, arXiv:2312.14693

Gautschy-Loidl, R., Höfner, S., Jørgensen, U. G., & Hron, J. 2004, *A&A*, 422, 289

Gonneau, A., Lançon, A., Trager, S. C., et al. 2016, *A&A*, 589, A36

Gray, R. O., & Corbally, Christopher, J. 2009, *Stellar Spectral Classification*

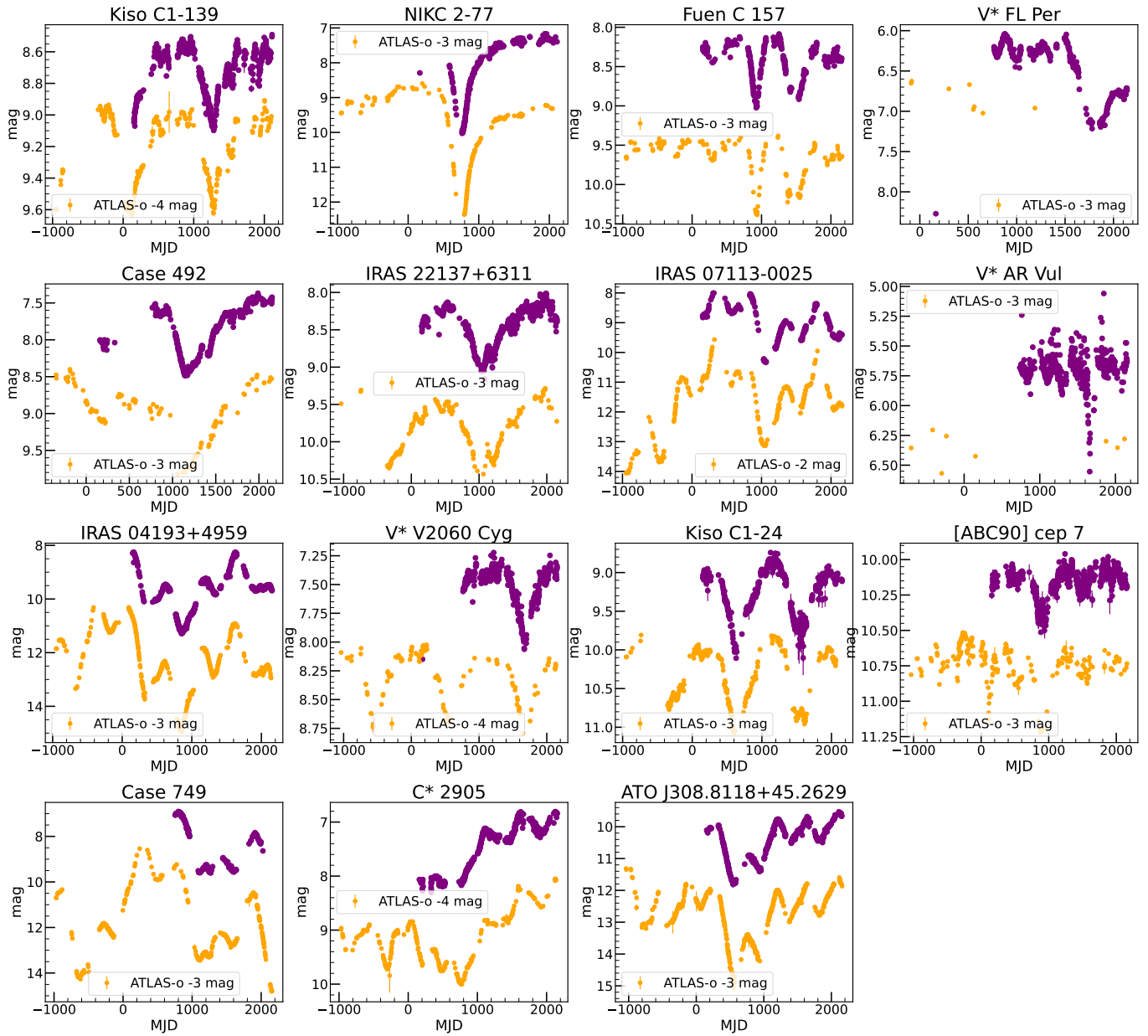


**Figure 12.** PGIR J-band lightcurves of candidate DY Per type stars

Green, G. M., Schlafly, E., Zucker, C., Speagle, J. S., & Finkbeiner, D. 2019, *ApJ*, 887, 93

Han, Z. 1998, *MNRAS*, 296, 1019

Herter, T. L., Henderson, C. P., Wilson, J. C., et al. 2008, in *Society of Photo-Optical Instrumentation Engineers (SPIE) Conference Series*, Vol. 7014, Proc. SPIE, 70140X

Karakas, A. I., Ruiter, A. J., & Hampel, M. 2015, *ApJ*, 809, 184

Karambelkar, V., Kasliwal, M. M., Tisserand, P., et al. 2022, *A&A*, 667, A84

Karambelkar, V. R., Kasliwal, M. M., Tisserand, P., et al. 2021, *ApJ*, 910, 132

Lamberts, A., Blunt, S., Littenberg, T. B., et al. 2019, *MNRAS*, 490, 5888

Lawson, W. A., & Cottrell, P. L. 1997, *MNRAS*, 285, 266

Lawson, W. A., Cottrell, P. L., Kilmartin, P. M., & Gilmore, A. C. 1990, *MNRAS*, 247, 91

Lawson, W. A., & Kilkenny, D. 1996, in *Astronomical Society of the Pacific Conference Series*, Vol. 96, *Hydrogen Deficient Stars*, ed. C. S. Jeffery & U. Heber, 349

Lee, C. H. 2015, *A&A*, 575, A2

Lee, C.-H., Matheson, T., Soraisam, M., et al. 2020, *The Astronomical Journal*, 159, 61



- Lee, O. J., Gore, G., & Bartlett, T. J. 1947, *Annals of the Dearborn Observatory*, 5, 287
- Lourie, N. P., Baker, J. W., Burruss, R. S., et al. 2020, in *Society of Photo-Optical Instrumentation Engineers (SPIE) Conference Series*, Vol. 11447, *Ground-based and Airborne Instrumentation for Astronomy VIII*, ed. C. J. Evans, J. J. Bryant, & K. Motohara, 114479K
- Maehara, H., & Soyano, T. 1987, *Annals of the Tokyo Astronomical Observatory*, 21, 293
- Maíz Apellániz, J., Holgado, G., Pantaleoni González, M., & Caballero, J. A. 2023, *A&A*, 677, A137
- Nassau, J. J., & Blanco, V. M. 1957, *ApJ*, 125, 195
- Otero, S., Hümmerich, S., Bernhard, K., & Sozynski, I. 2014, *Journal of the American Association of Variable Star Observers (JAAVSO)*, 42, 13
- Percy, J. R. 2023, *JAAVSO*, 51, 64
- Putney, A. 1997, *ApJS*, 112, 527
- Rayner, J. T., Cushing, M. C., & Vacca, W. D. 2009, *ApJS*, 185, 289
- Rayner, J. T., Toomey, D. W., Onaka, P. M., et al. 2003, *PASP*, 115, 362
- Ricker, G. R., Winn, J. N., Vanderspek, R., et al. 2015, *Journal of Astronomical Telescopes, Instruments, and Systems*, 1, 014003
- Saio, H. 2008, in *Astronomical Society of the Pacific Conference Series*, Vol. 391, *Hydrogen-Deficient Stars*, ed. A. Werner & T. Rauch, 69
- Schwab, J. 2019, *ApJ*, 885, 27
- Shields, J. V., Jayasinghe, T., Stanek, K. Z., et al. 2019, *MNRAS*, 483, 4470
- Smith, K. W., Smartt, S. J., Young, D. R., et al. 2020, *PASP*, 132, 085002
- Soszyński, I., Udalski, A., Szymański, M. K., et al. 2009, *Acta Astron.*, 59, 335
- Soyano, T., & Maehara, H. 1991, *Publications of the National Astronomical Observatory of Japan*, 2, 203
- Stephenson, C. B. 1973, *Publications of the Warner & Swasey Observatory*
- Tang, S., Cao, Y., Bildsten, L., et al. 2013, *ApJ*, 767, L23
- Tisserand, P. 2012, *A&A*, 539, A51
- Tisserand, P., Clayton, G. C., Welch, D. L., et al. 2013, *A&A*, 551, A77
- Tisserand, P., Crawford, C. L., Soon, J., et al. 2024a, *A&A*, 684, A131
- . 2024b, *A&A*, 684, A130
- Tisserand, P., Marquette, J. B., Beaulieu, J. P., et al. 2004, *A&A*, 424, 245
- Tisserand, P., Marquette, J. B., Wood, P. R., et al. 2008, *A&A*, 481, 673
- Tisserand, P., Wood, P. R., Marquette, J. B., et al. 2009, *A&A*, 501, 985
- Tisserand, P., Wyrzykowski, L., Wood, P. R., et al. 2011, *A&A*, 529, A118
- Tisserand, P., Clayton, G. C., Bessell, M. S., et al. 2020, *A&A*, 635, A14
- Tisserand, P., Crawford, C. L., Clayton, G. C., et al. 2022, *A&A*, 667, A83
- Tonry, J. L., Denneau, L., Heinze, A. N., et al. 2018, *PASP*, 130, 064505
- Vacca, W. D., Cushing, M. C., & Rayner, J. T. 2003, *PASP*, 115, 389
- von Neumann, J. 1941, *The Annals of Mathematical Statistics*, 12, 367
- Warner, B. 1967, *MNRAS*, 137, 119
- Webbink, R. F. 1984, *ApJ*, 277, 355
- Wong, T. L. S., & Bildsten, L. 2024, *ApJ*, 962, 20
- Zaniewski, A., Clayton, G. C., Welch, D. L., et al. 2005, *AJ*, 130, 2293
- Začs, L., Mondal, S., Chen, W. P., et al. 2007, *A&A*, 472, 247